Stony Brook University

Screening for Steroid-Derived Immunomodulatory Metabolites Biosynthesized by *Mycobacterium tuberculosis* (*M. tuberculosis*)

A Thesis Presented

by

Xiaoqian Jin

to

The Graduate School

in Partial Fulfillment of the

Requirements

for the Degree of

Master of Science

in

Chemistry

Stony Brook University

December 2012

Stony Brook University

The Graduate School

Xiaoqian Jin

We, the thesis committee for the above candidate for the

Master of Science degree, hereby recommend

acceptance of this thesis.

Nicole S. Sampson, Ph. D., Dissertation Advisor
Department of Chemistry

Erwin London, Ph. D., Chairperson
Department of Biochemistry and Cell Biology

Kathlyn A. Parker, Ph.D., Third member
Department of Chemistry

This thesis is accepted by the Graduate school

Charles Taber
Interim Dean of the Graduate School

Abstract of the Thesis

Screening for Steroid-Derived Immunomodulatory Metabolites Biosynthesized by *Mycobacterium tuberculosis* (*M. tuberculosis*)

By

Xiaoqian Jin

Master of Science

in

Chemistry

Stony Brook University

2012

Tuberculosis (Tb) is a serious worldwide threat to human health killing 1.4 million people every year. *Mycobacterium tuberculosis* (*M. tuberculosis*), the causative agent for Tb, has infected 30% of the world's population. The emergence of multidrug, extensively drug, and total drug resistant organisms (MDR/XDR/TDR TB) creates an urgent demand to develop new drugs with novel mechanisms to be effective against both sensitive and drug-resistant strains of *M. tuberculosis*. The cholesterol metabolism pathway in *M. tuberculosis* is important for mycobacterial survival in the host macrophage. We proposed that cholesterol serves as a starting material for biosynthesis of steroid-derived immunomodulators that down-regulate the host immune response in the intracellular environment. Therefore, identifying the metabolites, which are hypothesized to enable *M. tuberculosis* to modulate and evade the host immune response, can help elucidate the cholesterol metabolic pathways, presenting an attractive target for new drugs.

To determine whether *M. tuberculosis* produces immunomodulatory compounds that act as agonists or antagonists of nuclear receptors, our objective is to use bioassays to identify and isolate metabolites biosynthesized from cholesterol by *Mycobacterium Smegmatis (M.*

smegmatis). We set up the procedure for purification and analysis of low-density lipoprotein-cholesterol (LDL-cholesterol). By measuring the changes in fluorescence polarization, we also set up a screening assay for metabolites from *M. smegmatis* grown on LDL-cholesterol against glucocorticoid receptor.

Table of Contents

List of Figure

List of Tables

List of Schemes

List of **Abbreviation**

AD	Androst-4-ene-3,17-dione
ADD	Androst-4-diene-3,17-dione
AP-1	activator protein-1
$CHCl_3$	chloroform
DBD	DNA-binding domain
DMSO	dimethyl sulfoxide
EMB	ethambutol
EtOAc	ethyl acetete
Fad	fatty acid degrading
FP	Fluorescence Polarization
FRET	Fluorescence resonance energy transfer
GR	glucocorticoid receptor
H	human
HIV	human immunodeficiency virus
HPLC	high performance liquid chromatography
IC_{50}	half maximal inhibitory concentration
kDa	kilodalton
LBD	ligand-binding domain
LC	liquid chromatography
LDL	low density lipoprotein
LXR	Liver X receptor

M. smegmatis	*Mycobacterium smegmatis*
M. tuberculosis	*Mycobacterium tuberculosis*
MDR	multidrug-resistant
MeOH	methanol
mP	millipolarization
MR	mineralococorticoid receptor
MS	mass spectroscopy
NTD	N-terminal domain
OD	optical density
PBS	phosphate buffered saline
PZA	pyrazinamide
SDS-PAGE	sodium dodecyl sulfate polyacrylamide gel electrophoresis
Tb	tuberculosis
TCR	T cell receptor
TF	Transcription factor
TLC	thin layer chromatography
TLRs	Toll-like receptors
Tris	tris aminomethane
UV	ultraviolet
VDR	Vitamin D receptor
WHO	World Health Organization
XDR	extensively drug-resistant

Chapter 1. Introduction of *Mycobacterium Tuberculosis* and Steroid-derived Immunomodulatory Metabolites

Tuberculosis (Tb), which is caused by *Mycobacterium tuberculosis* (*M. tuberculosis*), is a serious worldwide threat to human health as a common and deadly contagious disease. It is estimated to have infected one third of the world's population, with 8.8 million new cases occurring each year, and 10% of *M. tuberculosis* infected individuals developing into active Tb infections.[1] In 2010, the World Health Organization (WHO) estimated that there were 9.4 million incident cases of Tb globally and approximately 1.7 million deaths.[2] Tb has become the infectious disease that kills more people than any other due to the emergence of virulent multidrug-resistant (MDR-TB) and, more recently, extensively drug-resistant (XDR-TB) strains of *M. tuberculosis*. In addition, Tb is the leading cause of death among individuals co-infected with HIV. There is an urgent demand to develop novel, effective, and efficient chemotherapies.

M. tuberculosis is an insidious pathogen that can remain latent for many years before becoming an active infection in the host. Because current antibiotics only target processes in active Tb infection, they are not effective in the treatment of slow growing or latent bacteria: Most Tb infections are in a latent phase competing for growth while persevering within the intracellular environment of the macrophage in host.[3] The balance between the host immune response and *M. tuberculosis* survival may be controlled by small molecules biosynthesized by *M. tuberculosis*. As a consequence, it is important to identify the immunoregulatory molecules

synthesized by *M. tuberculosis* that control the host immune system, which may also provide new targets for anti-infective therapy.

In this chapter, a brief overview of Tb, current treatments of the disease and challenges, steroid hormones biosynthesis in *M. tuberculosis* and their immunoregulation of Tb infection will be discussed.

1.1. *Mycobacterium tuberculosis*

Tuberculosis can be traced back to at least 20,000 years ago, with the discovery of *Mycobacterium tuberculosis (M. tuberculosis)* as the pathogen that is co-evolved with human beings.[4] Because no efficient treatment was available and its own mystery, Tb, for a long time, was known as "the white plague" or "consumption".[5] The first breakthrough was the discovery of *M. tuberculosis* as the pathogen of Tb, by Dr. Robert Koch, in 1882.[6] The method, using Bismarck brown staining and methylene blue, was developed into the well known Ziehl-Neelsen staining.[7] *M. tuberculosis* is classified as an acid-fast bacteria giving the fact that it does not give typical results by Gram staining.[8] Also, there are some other mycobacteria can cause mycobacterial infection in human beings, such as *Mycobacterium bovis, Mycobacterium microti,* and *Mycobacterium africanum,* which are not as common as *M. tuberculosis*.

1.2. *M. tuberculosis* infectious process

Tb is transmitted by small-particle aerosols from person to person, with the minimum infectious dose of one single bacterium.[9] In the majority of *M. tuberculosis* infections, the host

immune system phagocytoses the bacilli by alveolar macrophages, where the bacteria stay in a dormant state.[10] After the infectious bacilli are inhaled into the alveolar space, they start to replicate. This is the initiation of the infection as demonstrated by the *M. tuberculosis* life cycle. Following phagocytosis, *M. tuberculosis* could be killed by a series of mechanisms including phagosome-lyosome fusion, generation of reactive oxygen, and nitrogen intermediates and the innate immune response through antimicrobial peptide production. By evading these mechanisms, *M. tuberculosis* can survive and multiply within phagosomes.[11] Once inside the phagocyte, *M. tuberculosis* blocks fusion with acidic, hydrolytically active lysosomes modulating the activity of its mycobacterial phagosome.[12] Though it is still not proved clearly how phagolysosome fusion is arrested at molecular level, recent evidence suggests that it is a diterpene produced by *M. tuberculosis* that limits phagosomal maturation.[13] Avoiding lysosome fusion provides a chance for bacilli to replicate without activating macrophages. In this way, the bacilli survive and replicate in the vacuole spreading to other cells.[11]

In the classical view, this experimentally marks the beginning of exponential growth of the bacteria in macrophages, until the emergence of an inflammatory response resulting in the development of the granuloma, which means immune-mediated containment of the infection. It was reported that granuloma could proceed to localized sterilization of infection. Recent experiments revealed that the formation of granuloma precedes initiation of innate immune response[14]. The primary granuloma seeds disseminate second granulomas, which functions as spreading the infection instead of sequestering it.

In the following stage, a cell-mediated immune response occurs, which includes T-cell activation that can activate the macrophages in turn. The bacteria can colocalize with the cholesterol-rich region of the cell in the activated macrophage.[15] After that, the mycobacteria enter a bacteriostatic phase after the host is able to kill most of the bacteria and reduce the replication with macrophage activation. Then the infected macrophages are enclosed by foamy macrophages and lymphocytes, building a organized structure and vascularizing the granuloma[9]. In the further developed stage of granuloma, fibrous capsule becomes marked reducing the number of blood vessels. Meanwhile, noticeably foamy macrophages are forming. Both changes lead to the formation of caseum in the developed granuloma. In a case of progressive infection, along with the change in immune status, the center of the tubercle undergoes necrotic caseation and the infectious *M. tuberculosis* spills into other airways spreading the infection and completing the bacterium's life cycle (Figure 1-1).

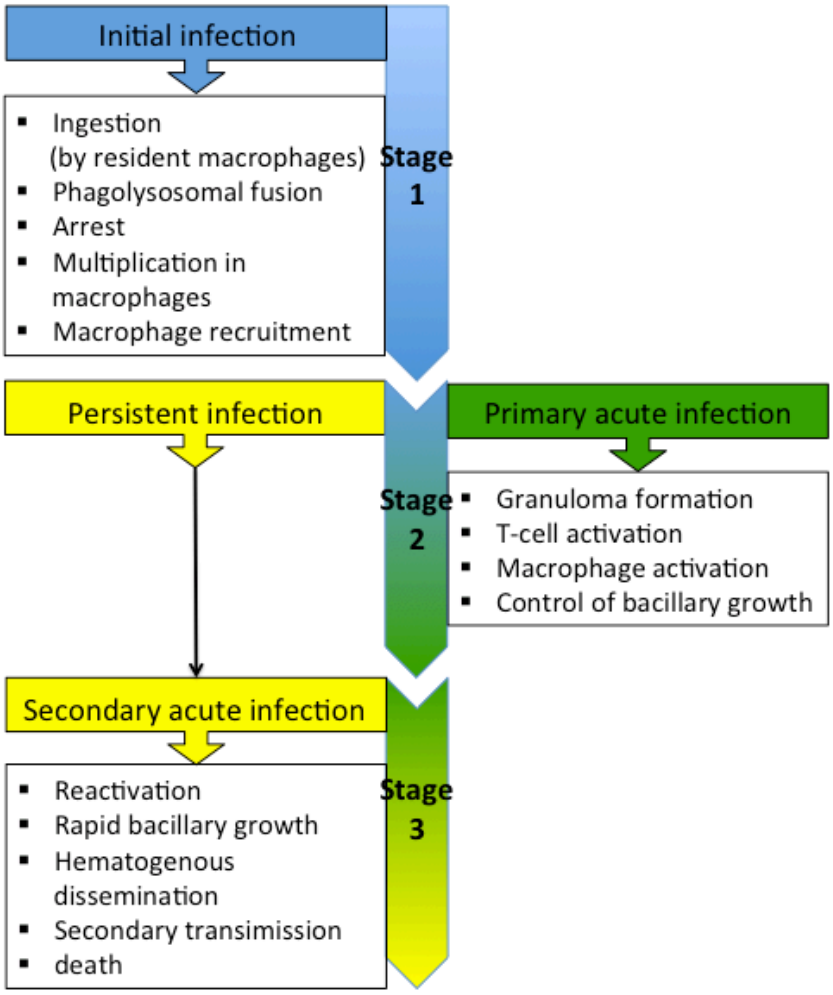

Figure 1-1. Stages of *M. tuberculosis* persistent infection[17].

In an *in vitro* model of human granulomas, it is also found that *M. tuberculosis*-derived lipomannan could drive the differentiation of granuloma macrophages into multinucleated giant cells, thus emphasizing the involvement of mycobacterial lipids in the modulation of the host response.[16] Given the life cycle of *M. tuberculosis*, it is implied that human immune system may be necessary for Tb to infect and spread.[17]

1.3. Current challenges in Tb treatment

There are three major current challenges for treating Tb: drug resistance, co-infection with HIV, and regimen non-compliance.

Current Tb therapies require a combination of multiple antibiotics for over six months, including a 2-month period using isoniazid, rifampicin, pyrazinamide (PZA), and ethambutol (EMB) or streptomycin, and another 4-month period of treatment with isoniazid and rifampicin. (Figure 1-2) The length of treatment causes difficulty in the compliance of the regimen. It has led to widespread multi-drug resistant Tb (MDR-TB),[18] which is tuberculosis that is, at least, resistant to the front-line Tb drugs: isoniazid and rifampicin; and the extensively drug-resistant tuberculosis (XDR-TB), which is tuberculosis that is resistant to these front-line treatments as well as at least one of the second line drugs.[19] As of 2008, 22 % of the new Tb cases were MDR-TB, with the rate of about 25,000 cases every year of XDR-TB emerging[20]. Because MDR-TB does not respond to the standard six-month treatment, it raises treatment as long as at least two years with drugs that are more toxic, more expensive, and less potent.[20a] The long treatment time is also the leading cause of non-compliance the treatment, which may, in return, result in greater drug resistance and Tb recurrence.[6, 21]

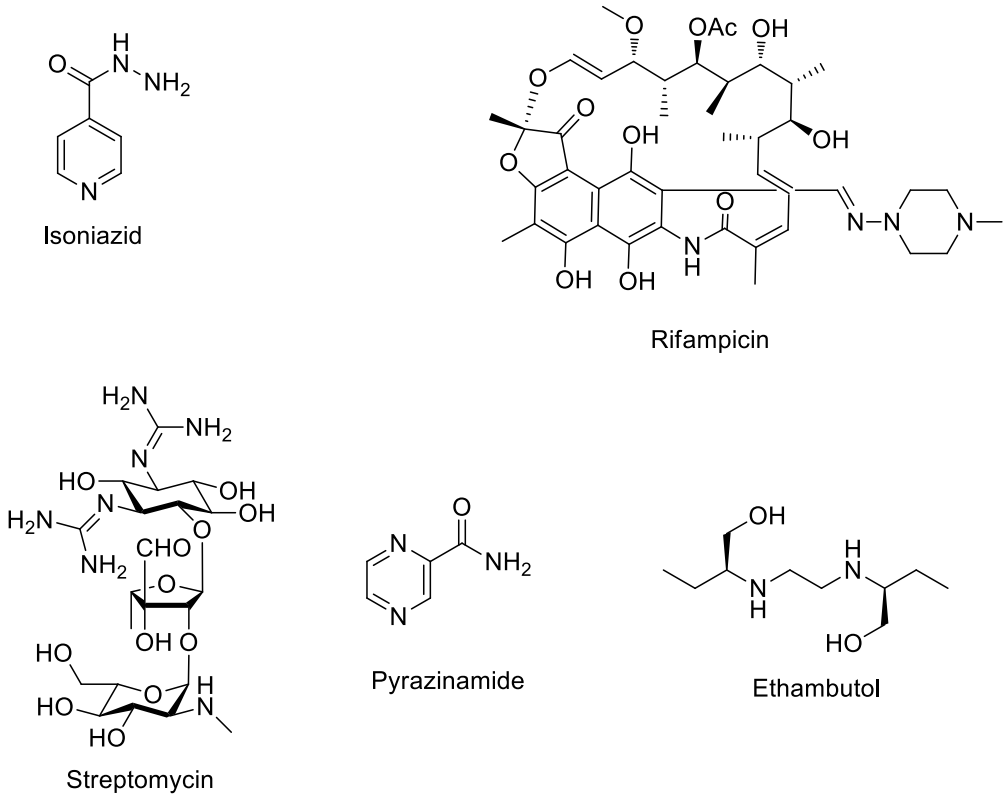

Figure 1-2. First-line antitubercular drugs.[22]

Due to coinfection with HIV, Tb has become the major reason for death among people with HIV.[22] In 2010, Tb caused 1.1 million cases of death among HIV-negative people and an additional 0.35 million cases of death among HIV-coinfected people.

1.4. Current treatment of Tb

For current Tb therapies, except for these first-line anti-Tb drugs, there are also some second-line anti-Tb drugs available for Tb chemotherapy, though they have lower efficiency and higher side effects. It has not been established well for the treatment of MDR or XDR-TB.[23]

The mechanisms of action of the antitubercular drugs are to target fatty acid biosynthesis, protein synthesis, DNA expression, and peptidoglycan biosynthesis. Isoniazid, for example, targets InhA, an acyl-carrier protein reductase, preventing the synthesis of the bacterium cell wall. Another front line drug, which is a group of natural or semi-synthetic antibiotics, binds to the β-subunit of the DNA-dependent polymerase[24]. Streptomycin, which belongs to aminoglycosides, targets the 30S subunit of ribosome leading to the mistranslation of mRNA.[25]

A proper guideline for Tb treatment has become a difficult but urgent task. Several aspects, including bacteria strains, patients' physiological conditions, and progression of disease, should be taken into consideration to adjust the treatment for different cases.[26]

1.5. *M. tuberculosis* and cholesterol

Foamy macrophages are lipid-rich, consisting of cholesterol, cholesterol ester, triacylglycerides, and phospholipids. In foamy macrophages, *M. tuberculosis* is found closed to lipid bodies under electron microscopy.[27] It has been observed that fatty acids rather than carbohydrates are able to stimulate respiration within the mouse lung, which indicates that, during chronic infection, *M. tuberculosis* switches to using those lipids as a carbon source. Moreover, the isocitratelyase (Rv0467), an enzyme essential for fatty acid metabolism, is required for the persistence of the bacteria.[28] It has been supported by the study that the genome of *M. tuberculosis* contains a large number of genes, approximately 250, that are annotated as being involved in lipid and fatty acid metabolism.[29]

It has also been revealed that, *in vivo*, foamy macrophages contain high levels of cholesterol esters, and it is highly possible that the lipid bodies that merge with *M. tuberculosis* are composed of cholesterol esters.[30] Transcriptional profiling experiments on bacteria have demonstrated that many of the hypothesized lipid metabolizing genes are required for bacterial cholesterol utilization during the infection of macrophages and mice.[31] Moreover *M. tuberculosis* is able to import cholesterol via the ABC transporter Mce4.[32] This transporter is critical for *M. tuberculosis's* ability to use cholesterol and is necessary for persistence of the bacteria, implicating the important relationship between *M. tuberculosis* and cholesterol.

The role of cholesterol metabolism by the bacteria is not clear, and neither is the role of cholesterol during infection. In the intracellular environment, *M. tuberculosis* shifts from a carbohydrate to a fatty acid-based metabolism.[33] In culture, *M. tuberculosis* grows on cholesterol, which is soluble in tyloxapol, as the sole carbon source. The results of ^{14}C-labeling experiments indicate that the C4 in ring A is converted to CO_2 while C26 in the side chain is incorporated into mycobacterial lipids (Figure 1-3). In culture, the growth curve reaches stationary phase at a much lower cell density on cholesterol comparing with the growth curve of growth on glycerol. The limited growth suggests growth inhibition may occur as a consequence of cholesterol metabolism, explaining the difficulties of growing *M. tuberculosis* on plates using cholesterol as the only carbon source.[34]

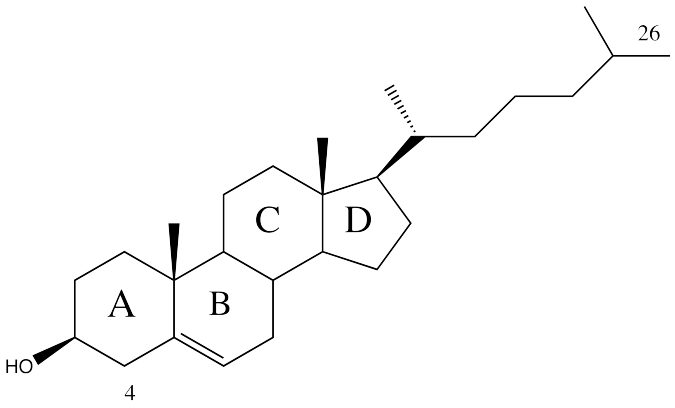

Figure 1-3. Cholesterol with C4 and C26 atoms indicated.

Lack of proper experimental *M. tuberculosis* models that provide a mechanistic understanding of *in vivo* conditions hinders a better understanding of the infection process.[27] Not only is it difficult to work with *M. tuberculosis* because of its slow growth rate, but most *in vitro* models are inaccurate simulations of *in vivo* conditions. *In vivo* animal models can better characterize the disease, though with less control over experimental conditions. The first direct evidence suggesting that the bacterial cholesterol metabolism is necessary for *M. tuberculosis* survival *in vivo* is from a study of a Mce4 ABC transporter mutant, which is defective in cholesterol transport.[35] The *M. tuberculosis* mutant had a reduced ability to catabolize cholesterol and a slowed uptake of cholesterol. The mutant was unable to replicate in activated macrophages or in the mouse model of infection; growth sharply slowed in the chronic phase.[15]

1.6. Steroid hormone biosynthesis

In vivo, mycobacteria have access to abundant cholesterol, a likely starting material for mycobacterial biosynthesis. Based on elucidated metabolite structures, the pathway for cholesterol degradation in *M. tuberculosis* has been proposed (Scheme 1-1).

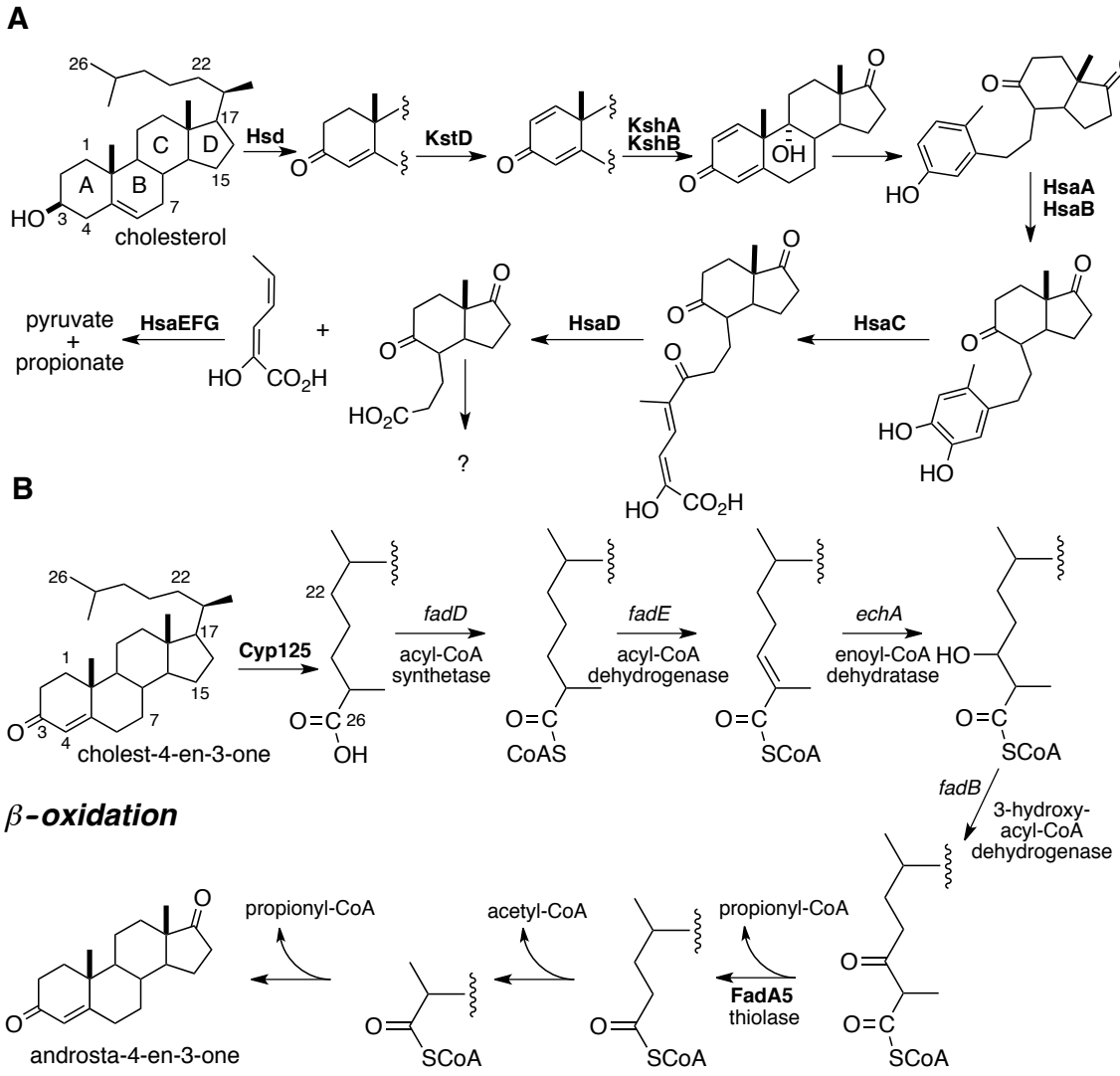

Scheme 1-1. Proposed cholesterol degradation pathway.[16]

A key step early in the mammalian hormone biosynthesis pathways is the oxidation and isomerization of a 3β-hydroxy steroid by a 3β-hydroxysteroid dehydrogenase. The biochemical functions of many annotated steroid-metabolizing genes in *M. tuberculosis* have not been verified with gene product. However, the *M. tuberculosis* gene (*Rv1106c*) coding for this enzyme has been identified establishing its enzymatic activity.

Previously, our group isolated wild-type secreted metabolites of cholesterol in an investigation of the role of the *fadA5* gene in cholesterol metabolism. In mice infected by the aerosol method, the *fadA5* mutant initially grew at the same rate as the wild-type strain. After 8 weeks, the number of bacteria in mice lungs decreased because of the immune response. The complementation of *fadA5* restored growth to the level of wild-type strain. This indicated that at the early stage of *M. tuberculosis* infection, cholesterol is not the only carbon source before immune response.

Our lab has isolated wild-type secreted metabolites of cholesterol during our investigation of the role of the *fadA5* gene in cholesterol metabolism.[35] We grew cultures of H37Rv, the *fadA5* mutant, and the complemented *fadA5* mutant in complete medium to the logarithmic stage of growth. Cholesterol was added to the cultures, and 48 hours later, lipids of both cell pellets and culture supernatants were extracted. The extracts were analyzed using ultraviolet-visible spectroscopy (UV), mass spectroscopy (MS) and liquid chromatography (LC). The wild-type strain secreted two metabolites into culture supernatants, androst-1,4-diene-3,17-dione (ADD) and androst-4-ene-3,17-dione (AD), which were absent in the *fadA5* mutant cultures. The λ_{max} of the two metabolites are 245 nm and 243 nm, while the one with MH^+ parent ions are at 285.2 nm and 287.2 nm. The spectroscopic data as well as the retention times were consistent with the prediction of metabolites ADD and AD, suggesting that complementation of the *fadA5* mutant strain restored production of ADD and AD.

Both the *in vitro* and *in vivo* experiments suggest that producing steroid metabolites during the chronic phase of infection is a critical role of cholesterol metabolism by *M.*

tuberculosis. These studies demonstrated that wild-type *M. tuberculosis* can produce androgens that function as weak immunomodulators.[36]

1.7. Immunoregulation in tuberculosis

Experimental data accumulated over that past 20 years support the importance of physiological interactions between hormones and immune systems[37]. Immune regulators cannot function in isolation—complex physiological interactions are necessary and essential for efficient immune homeostasis.[37-38] In mammalian biosynthetic pathways, steroid-derived hormones, such as cortisol and calcitriol, are synthesized from cholesterol.

Glucocorticoids (GC), e.g., cortisol or dexamethasone, are known to have complex immunoregulatory functions.[39] They function as immunosuppressive, anti-inflammatory steroids via inhibition of transcription factors involved in regulation of cytokines, such as the nuclear factor of activated T cells (NFAT), activator protein-1 (AP-1), and nuclear factor kB (NF-kB). In this way, they can reduce T-cell proliferation. Moreover, cortisol can regulate the biosynthesis of enzymes that are important for the action of macrophages. Glucocorticoid immunoregulation is orchestrated by specific binding of GCs on two cytoplasmic receptors, which are the mineralocorticoid receptor (MR) and the glucocorticoid receptor (GR). Although the MR has a higher binding affinity for circulating GCs than the GR, most, if not all, effects on the immune system are mediated by GRs making GR central to the immunomodulatory effects.

Another immunoregulator steroid, Vitamin D, also plays an important role in the protection against respiratory infection. Evidence shows that as far back as the early 20th century,

one treatment for *M. tuberculosis* is to provide high levels of sun exposure to increase the bioavailability of Vitamin D. Recently, it has been confirmed by epidemiological studies that the risk of tuberculosis in patients increased with Vitamin D deficiency.[40] Vitamin D, calcitriol, which binds to the nuclear Vitamin D receptor (VDR), can be found in immune cells. Also the activation of Toll-like receptors (TLRs) triggers a microbiocidal pathway as part of the innate immune response to *M. tuberculosis* leading to killing of intracellular bacteria.[41] It has been reported that the activation of TLR2 and TLR1 heterodimer (TLR2/1) includes calcitriol production and VDR upregulation.[42] Thus, calcitriol regulates the biosynthesis of antimicrobial peptides.

The utilization of glucocorticoid for treatment of inflammatory diseases can increase the risk of infection with intracellular pathogens, such as *M. tuberculosis.*[43] Reducing vitamin D levels can contribute to increased susceptibility to *M. tuberculosis* infection.[44] In this way, agonism or antagonism of the GR or VDR by *M. tuberculosis* synthesized molecules could lead to host immune suppression and increased *M. tuberculosis* survival in the host immune system.

The LXRα, androgen, and FXR nuclear receptors, which bind steroid agonists, may also be targeted by *M. tuberculosis*, although their functions have not been shown to be involved in *M. tuberculosis* infection. The nuclear-receptor superfamily has various and critical roles in regulating developmental, homeostatic, reproductive, inflammatory, immune, and metabolic processes.[45] The Liver X Receptors (LXRα and LXRβ), which are members of the nuclear receptor superfamily, are lipid-activated transcription factors that regulate cholesterol homeostasis.[45-46] LXRα is highly expressed in liver, adipose tissue, and macrophages. Recent

studies have suggested that LXR function as a negative regulator of inflammatory gene expression via transrepression.[47] Interestingly, the inhibition of LXR cholesterol function, activated by TLR3 or TLR4, occurs via the transcription factor IRF-3, supporting the hypothesis LXR regulates crosstalk between metabolic and inflammatory pathways.[48] It is the ability of these nuclear receptors to integrate metabolic and inflammatory signaling that makes them attractive targets for intervention in human metabolic diseases, as well as the modulation of inflammation and immune responses.[46] Conversely, *M. tuberculosis* may target them to evade from the human immune system.

1.8. Screening for steroid-derived immunomodulatory metabolites biosynthesized by *Mycobacterium smegmatis*

In order to study the small molecules that are involved in *M. tuberculosis* infection, our long-term goal is to elucidate the *M. tuberculosis* cholesterol metabolic pathways. In this project, our objective is to set up a high-throughput screening against the metabolites that are biosynthesized by *Mycobacterium smegmatis* (*M. smegmatis*) during growth on cholesterol. We hypothesized that cholesterol can serve as a starting material for the biosynthesis of host immunomodulators. The specific aim is to identify candidate immunomodulatory metabolites, which can act as agonists or antagonists of glucocorticoid receptors, produced during the growth of *M. smegmatis* on LDL (low-density lipoprotein)-cholesterol.

Using fluorescence polarization, we will screen *Mycobacterium smegmatis* samples against the glucocorticoid receptors. *M. smegmatis* is a popular model system for *M. tuberculosis*, since it is not pathogenic and has a faster growth rate. Being found in soil and

water, *M. smegmatis* has capability of growing in most of laboratory media. Moreover, it has been indicated that *M. smegmatis* shares genomic fragments with *M. tuberculosis* with conserved cholesterol region.

In our study, we chose LDL-chol instead of cholesterol itself, because cholesterol is hydrophobic making it hardly able to dissolve in most laboratory media or water. However, adding detergence to dissolve cholesterol can bring a lot of extra possible influences on the results of the experiment. LDL complex, which is coated with apoprotein B-100, is soluble in water. Moreover, it has been proved that LDL-cholesterol complex is the main source for cell to get cholesterol *in vivo*.

Our experimental strategy is to prepare cultures of *M. smegmatis*, screen extracts of cell pellets and culture supernatants for binding to glucocorticoid receptors, fractionate the extracts, isolate the active components, and determine their molecular identity.

The reason we start from the glucocorticoid receptors is it has been reported that these receptors have important roles in the immune regulation of *M. tuberculosis* infection.[41, 44] We are also interested in vitamin D, LXRα, androgen, and FXR receptors because of the evidence that they can be activated by sterol metabolites and can play a role in human immune response.[37, 46]

1.8.1. Glucocorticoids and glucocorticoid receptor

In humans, glucocorticoids (GCs) are steroidal hormones, which regulate a series of physiologic functions that play essential roles for life, enabling the responses of organism to adapt to the physical or emotional stress.[49] Synthesized from cholesterol, GCs are named after their roles in regulation of glucose metabolism, the synthesis in the adrenal cortex and the steroidal structure: glucose+cortex+steroid. Glucocorticoids regulate approximately 20% of total gene expression in human leukocytes, positively or negatively.[50]

Glucocorticoids can induce the breakdown of proteins into amino acids as well as stimulate the mobilization of fatty acid. They antagonize the function of insulin, in humans, being categorized as "catabolic" hormones. GCs can decrease the use of glucose to increase the levels of blood glucose. Most importantly to our project, GCs have immunoregulations and functions of immunomodulators making them promising as the targeted treatment study.

At the cellular level, glucocorticoid action is principally mediated via an intracellular protein, the glucocorticoid receptor (GR).[51] The full-length human (h) GR protein, which belongs to the steroid acid nuclear receptor superfamily of transcription factor, comprises 777 amino acids (Figure 1- 4A). hGR regulates the expression of glucocorticoid-responsive genes as a ligand-dependent transcription factor. The hGR gene is located on chromosome 5 consisting of nine exons. It is alternatively spliced into two homologous receptor isoforms, hGRα and hGRβ. They are highly identical with only 50 additional amino acids in hGRα and 15 nonhomologous amino acids in hGRβ (Figure 1- 4B). Residing in the cytoplasm of cells, hGRα, which is the

classic GR, functions as a ligand-dependent transcription factor; while hGRβ, without binding GCs, exerts dominant and negative functions on the transcriptional activity of hGRα.

The human GR comprises an N-terminal domain (NTD), a conserved DNA-binding domain (DBD), and a C-terminally localized ligand-binding domain (LBD) (Figure 1- 4A).[49, 52] The NTD of hGRα, which is ligand-independent, plays an important role in transcription factor interactions and cofactor interactions, containing a major transactivation domain. The DBD of hGRα, which corresponds to amino acids 420-480, is the most highly conserved domain in the steroid receptor family containing two zinc finger motifs. It is involved not only in specific DNA binding, but also in interaction with other transcription factors, nuclear location, and dimerization. The LBD of hGRα, which corresponds to AA 481-777, is necessary for ligand-induced activation of hGRα, transactivation functions, and nuclear localization functions. LBD plays a critical role in enabling GR to perform as a true transcription factor and favoring nuclear localization other than nuclear export, given the conformational change of the receptor during ligand-binding.[52]

A.

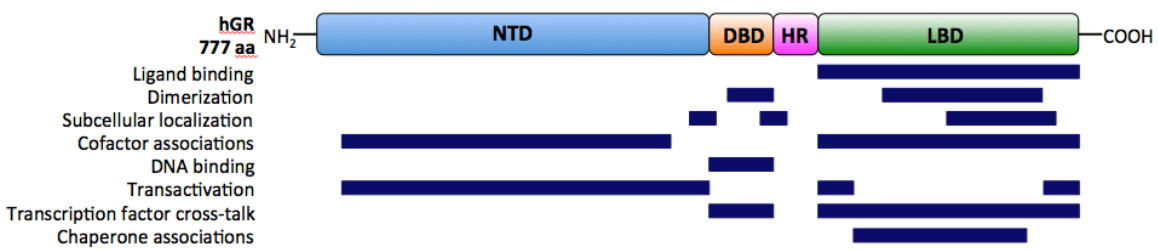

B.

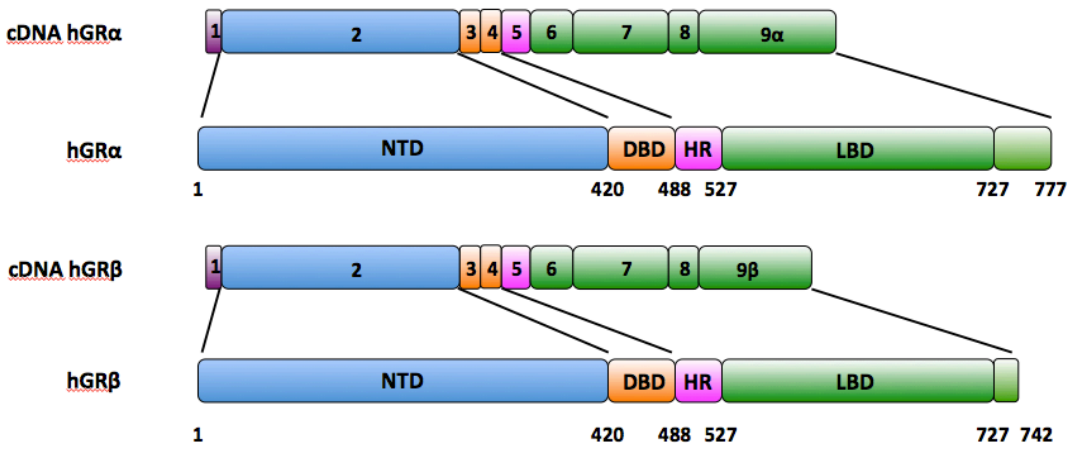

Figure 1-4. The structure of the glucocorticoid receptor gene and protein.

The crystal structure of the ligand-binding domain of hGRα 12 α-helices and 4 β-strands folding into a three-layer helical domain.[51a] Helix (H) 11 and Helix (H) 12 played important roles in determining the agonist or antagonist forms. When H12 adopts a position over the ligand-binding pocket, hGR is in the agonist-bound conformational state, forming an active receptor for transcription. On the other hand, when the structural changes unfold the C-terminal portion of H11 unfold the helix and H12 moves over the ligand-binding pocket, the protein is in the antagonist form.[51a]

The transcriptional activities of hGR can be classified into three major modes: transactivation, cross-talk interaction with other transcription factors, and nucleocytoplasmic shuttling of hGR. By direct binding to glucocorticoid responsive elements (GREs), GR can support transactivation; while, instead of binding to DNA, when the activated GR interferes with other DNA-bound transcription factors (TFs), another form of gene regulation will occur by cross-talk mechanisms. Different modulators for GR lead to different transcriptional

consequences. The slight differences of GR modulators, for example a ligand with more dissociated profile (Ligand A) and the classic ligand (Ligand B) can induce different GR structures, which results in inactivating of different kinase pathways. Furthermore, different GCs can influence the receptor retention time on DNA, which may result in the different selectivity of transcription factors influencing the transcriptional outcomes. It has also been reported that the differences between GREs can contribute to the differential transcriptional behavior of ligand-binding and GR dimerization. Being modulated differently into different structures, the receptors will be surrounded by different cofactor, for example in state of transactivation or transrepression. All in all, hGRα isoforms may transduce the signal of glucocorticoids to target tissues differentially.

Research studies on genomic GR effects indicate that alterations in hGR action probably have critical implications for many biological processes, such as the immune and inflammatory reaction, the growth and reproduction, and the physiologic responses to stress.

Among the multiple functions of hGR, the nongenomic mode of action in T cells elucidated a novel mechanism for GC action indicating the unexpected role as regulators of T cell receptor (TCR) for membrane GR. *In vitro*, using dexamethasone (Dex), it has been revealed that GC can inhibit TCR signaling. It was shown that Dex binds to membrane-bound GR leading to the inhibition of TCR signaling. These results indicate that GR is a promising therapy target for tuberculosis to develop novel class treatment using steroids-derived compounds. This will enable the immune system itself to find the bacteria and kill it, solving the problem of drug resistance.

1.8.2. Fluorescence polarization

Fluorescence Polarization (FP) measurements, first described by Perrin have become a widely-used assay format for homogeneous, solution-based analysis of molecular interactions in biological and chemical systems.[53] Different from fluorescence techniques, FP depends on changes in the apparent size of the fluorescent or fluorescently labeled molecules rather than changes of intensity or wavelength, making FP assays easy to be developed. Without any separation or purification steps, FP is possible to monitor molecular binding events in solution.[54] Other fluorescence techniques, such as fluorescence resonance energy transfer (FRET), which are also homogeneous, require multiple labeling reactions; while FP works with crude and unlabeled receptors.[55] Also, being non-destructive, FP allows repetitive measurements of the same sample under different conditions. Due to its sensitivity, speed, ease of use, and cost effectiveness, FP has become a useful, powerful, and popular technique for various fields of studies, such as the detection of drugs, therapeutic drug monitoring, environmental monitoring, and diagnostic applications for infectious diseases.

The principles of FP depend on the excitation of a fluorescent molecule with plane-polarized light (Figure 1-5). FP measures changes in orientation of plane-polarized light brought by fluorescent compounds during the fluorescence lifetime of the fluorophores. The lifetime is the period of time between absorption of an excitation and emission photon though fluorescence. A fluorophore whose absorption vector is aligned with polarized excitation light is selectively excited. If the fluorophore rotates rapidly relative to its fluorescent lifetime it will be randomly orientated prior to light emission and resulting a low polarization value (Figure 1- 5A). However,

if this fluorophore's rotation is slow so respect to the fluorescent lifetime it will not rotate much before light emission and will result in a high polarization value (Figure 1- 5B).[56]

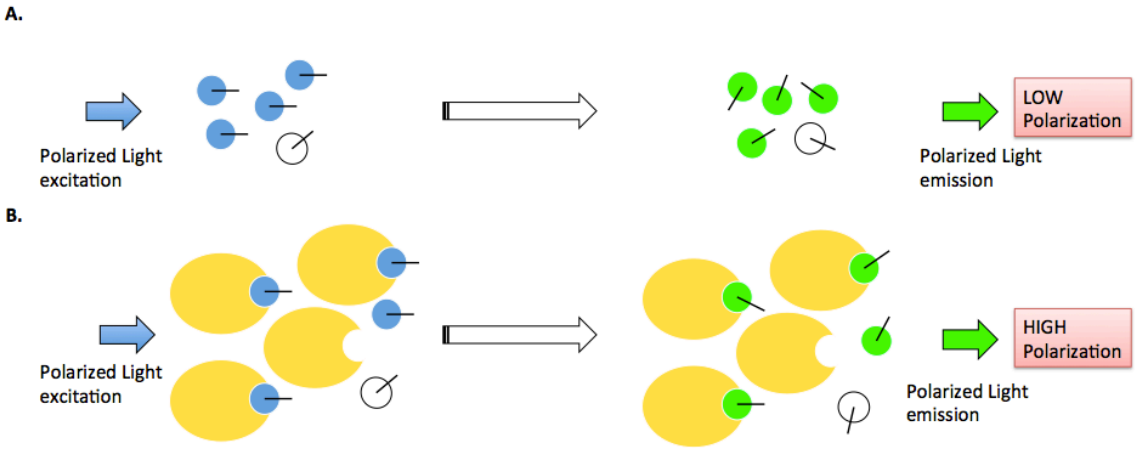

Figure 1-5. Principle of fluorescence polarization.

Plate reader measures the light emitted from a fluorescent ligand in two planes (horizontal and vertical) after excitated with plane-polarized light (Figure 1- 6). Excitation light passes through excitation and polarization (horizontal) filters and is then reflected by a dichroic mirror to the sample. Emitted light passes through a dichroic mirror to the sample.

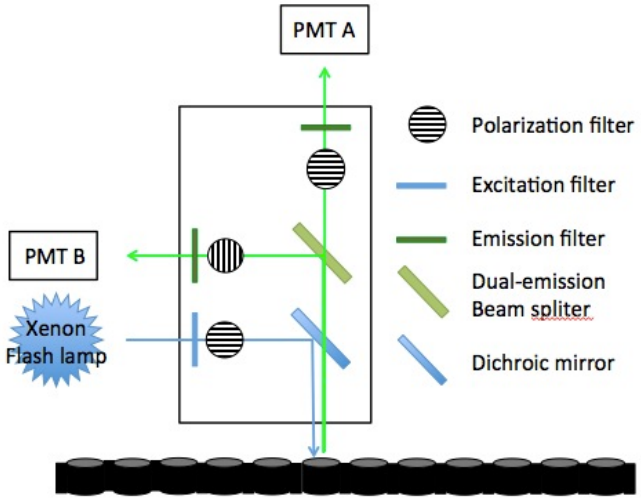

Figure 1-6. Ligand binding analyzed by fluorescence polarization.

Data are obtained for the fluorescence perpendicular to the excitation plane (the "P-channel") and fluorescence that is parallel to the excitation plane (the "S-channel"). For screening applications, the millipolarization units (mP) are often calculated using:

$$mP = 1000 \times \left(\frac{P - (G \bullet S)}{P + (G \bullet S)} \right) \qquad \textbf{Equation 1.}$$

In order to use S and P channel data properly, a correction is necessary to measure the absolute polarization state of the molecules. Thus the value of the instrument "G-factor", which stands for "grating-factors", needs to be measured and calculated. This correction factor can be constantly applied to both parallel and perpendicular channels, though it is more applied to measurement of the perpendicular channel. The value of G-factor has been determined by Equation 2.

$$G = \left(\frac{average(P)}{average(S)} \right) \left(1 - \frac{27}{1000} \right) \qquad \textbf{Equation 2.}$$

1.8.1. Receptor-binding assays

Receptor-binding FP assays use a small molecule labeled ligand and a large unlabeled receptor. This type of assay usually yields a minimum signal of approximately 50 mP for the free ligand and a maximum signal of approximately 300 mP when the fluorescent-labeled ligand is bounded to the receptor.

In our project, the assays for direct binding to nuclear receptors use purified untagged glucocorticoid receptors in cell-free system. This spectroscopic assay measures whether a ligand is directly binding to the receptor by fluorescent ligand displacement. Upon competitive displacement of a fluorescent dexamethasone, or calcitriol derivative by metabolites, fluorescence polarization decreases. The assay does not distinguish whether the metabolites can activate or antagonize the receptors. However, it provides information about the efficacy of binding to the ligand-binding domain directly.

The Glucocorticoid Receptor (GR) competitor assay is one of the receptor-binding assays. The GR, Green kit provides a sensitive and efficient method for high-throughput, fluorescence polarization-based screening of potential glucocorticoid receptor ligands, which is also commercially available from Invitrogen. The kit uses an insect cell-expressed, full-length, untagged, human glucocorticoid receptor (GR) with a novel, tight-binding, fluorescent-labeled ligand (Fluormone GS1) in a homogenous mix-and-read assay format (Figure 1-7). GR is added to a fluorescent glucocorticoid ligand, Fluormone GS1, in the presence of individual test

compound in 96-well plates. If a test compound does not compete with Fluormone GS1 for binding to the GR, then the GR/Fluormone GS1 will rotate slowly during its fluorescence lifetime, resulting in a high polarization value; while if a test compound does compete with Fluormone GS1, the GR/Fluormone GS1 will tumble rapidly, resulting in a low polarization value. The changes in polarization values are used to determine the relative affinity of the test compound for GR.

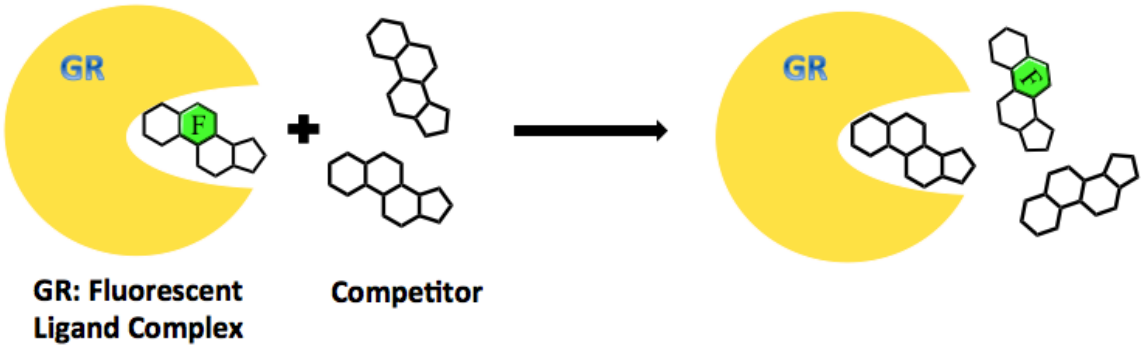

Figure 1-7. The theory of glucocorticoid receptor competitor assay.

Chapter 2. Experimental Section

2.1. Purification of low-density lipoprotein (LDL) from egg yolk

2.1.1. Plasma fractionation and LDL extraction

Fresh chicken eggs were collected. The eggs were manually broken and yolks were separated from the albumen. Each yolk was carefully rolled on a filter paper (Whatman, Springfield Mill, England) to remove chalazae and albumen adhering to the vitellin membrane. The vitellin membrane was disrupted with a scalpel blade and the unspoiled egg yolk was collected in a beaker cooled in iced water after washing 2 times with phosphate buffered saline (PBS).

Yolk was fractionated into plasma and granules according to the method described by McBee and Cotterill.[54] Yolk was diluted with two times of the yolk volume of an isotonic saline solution (0.17 M NaCl) and stirred with a magnetic stirrer for 1 h at 4 °C. Then, the solution was centrifuged at 10,000 × g for 45 min at 4°C. The supernatant was centrifuged again with the same condition. In this way the sediment (granules) were completely removed and the supernatant (plasma) was separated from the granules. Plasma was then conserved at 4 °C for further extraction.

40% Ammonium sulfate (Sigma-Aldrich Chemie, Steinheim, Germany) was added to the plasma stirring for 1 h at 4 °C to precipitate livetins. The pH of the plasma was fixed and controlled at 8.7 and centrifuged at 10,000 × g for 30 min at 4 °C to separate the supernatant

from sediment. The precipitate was discarded and the supernatant was dialyzed at least 6 h against distilled water (3000 mL) to eliminate ammonium sulfate (Sigma-Aldrich, Germany), changing the dialysate every 2 h. After complete ammonium sulfate elimination, the solution was again centrifuged at 10,000 × g for 30 min at 4 °C. The floating residue, rich in LDL, was collected.

Dry matter was collected and determined after lyophilization for 48 hours. Rotovap or Centricon (MWCO 10k) was employed to concentrate the solution before freeze-drying.

2.1.2. Chemical analysis of the LDL-cholesterol

TLC

The sample was dissolved in chloroform. A standard of cholesterol (Sigma-Aldrich, Germany, 95%) in chloroform were prepared as 10^6 nM. They were run on TLC eluting with a mixture of hexane and ethyl acetate with a ratio of 1:1.

SDS-PAGE

Protein composition and the relative quantity of apoproteins from LDL were analyzed by SDS-PAGE. Samples were dissolved in 5× sample buffer: 1M Tris-HCl (Sigma-Aldrich, Germany), pH=6.8; 50% glycerol; 10% SDS (Sigma-Aldrich, Germany) solution; 2-mercaptoethanol 0.5 ml; 1% bromophenol blue; distilled water. The mixture of samples and buffer was plunged for 5 min in boiling water. The stacking and running gels were 3.5% and 10% polyacrylamide, respectively. The migration buffer consists of 0.1 M Tris-HCl (pH 8.8),

tricine 0.1 M, and SDS 0.1% solution. Approximately 20 μg of proteins were loaded on the gel. The protein ladder was also loaded on the gel. Electrophoretic migration was performed at 80 V for 0.5 hour followed by 1 hour. The proteins were stained with Coomassie blue: 0.05% Coomassie blue, ethanol 25%, acetic acid 10%, ethanol 40%, and water 53%. After destaining, the gels were then scanned into images for documenting.

Total cholesterol oxidation assay

In order to determine the amount of cholesterol in LDL, a total cholesterol oxidation assay were set up employing UV-Vis spectroscopy. Starting from set up cholesterol oxidation assay, a stock solution of cholesterol was prepared by dissolving cholesterol in propan-2-ol with Triton's stirring for 2 h. This solution was filtered through a 0.45 μ nylon filter. To make a standard cholesterol oxidation curve, the absorptions were measured by the differences between the appearance of cholest-4-en-3-one at 240 nm (ε_{240} =12100 M^{-1} cm^{-1}) and the 50 mM sodium phosphate buffer, pH= 7.0, at 37 °C, with respect to different concentrations of the cholesterol. The standard assay conditions were run in the same buffer. Different volumes of cholesterol stock solution were with the same amount of oxidase to obtain different total changes in absorbance. With the standard curve, we applied the cholesterol oxidation assay to the LDL. And in this way, the concentration of free cholesterol was measured. After that, the concentration of total cholesterol was measured by incubating the LDL with esterase for 30 minutes before adding the oxidase.

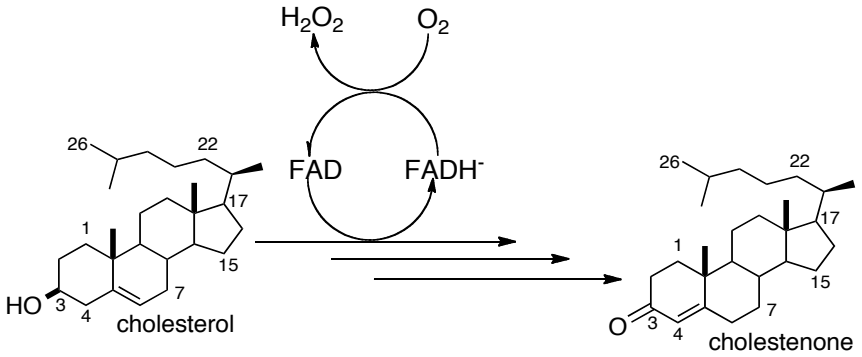

Scheme 2-1. Oxidation of cholesterol into cholestenone.

The activity of cholesterol oxidase was also measured by following the absorption at 505 nm by coupling to peroxidase. In order to determine the concentration of total cholesterol in LDL, different amounts of 4.4 mg/mL cholesteryl acetate in isopropanol were added into master batch, including 0.7 nM 4-amonoantipyrine in 0.1 M phosphate buffer (14 mL), 5.0 mM phenol in 0.1 M phosphate buffer (14 mL), 0.351g sodium cholate in DDI water (1 mL), 1 mL 5% Triton X-100, 8200 unit/ml peroxidase (0.64 mg), and 69 μM cholesterol oxidase (60 μL). After incubating for 0.5 hour, 8 mg/mL esterase (50 μL) was added into each cuvette. The concentration of the total cholesterol in LDL was determined by applying the standard curve.

$$2H_2O_2 + \text{4-AAP} + \text{Phenol} \xrightarrow{\text{Peroxidase}} 4H_2O + \text{Quinoneimine Dye}$$

Scheme 2-2. Peroxidation producing quinoneimine dye from 4-AAP

2.2. Bacterial strains, media, and conditions

M. smegmatis cultures were grown at 37 °C in Middlebrook 7H9 liquid media, supplemented with 0.2% glycerol for 48 h, or on Middlebrook 7H10 plates supplemented with glycerol. The cultures were scaled up from 1 mL to 500 mL, step by step, with 10 times dilutions. Antibiotics were added at 100 μg/mL of ampicillin and 10 μg/mL of cycloheximide. The bacteria were resuspended in 7H9 liquid media supplemented containing LDL-cholesterol (50-60 μg/mL) of culture. Treatment with only glycerol was used as a negative control. Cultures were harvested by centrifugation. The cell pellets and the sterile filtered culture supernatants were collected and stocked for further analysis.

Lipid extractions

Cell pellets were extracted by the Bligh-Dyer method[57] (for each 1 mL of sample, 3.75 mL 1:2 (v/v) $CHCl_3$: MeOH and vortex well; following with 1.25 mL $CHCl_3$ and 1.25 mL dH_2O), concentrated to dryness and resuspended in ethyl acetate (EA).

The culture supernatants were extracted with EA (300 mL) twice. The aqueous layers were acidified to pH 5 and extracted with EA (300 mL) twice. The organic layers were combined and washed with H_2O three times and concentrated. The supernatants and cell pellets either from glycerol or LDL-cholesterol cultures were dissolved in DMSO, or methanol for the assays.

2.3. Glucocorticoid receptor competitor assay

In order to correct the value of mP, the fluorescence polarization test assay were run several times to measure the value of "G-factor" by using the FP One Step Reference Kit.

The assay is commercially available from Invitrogen. Fluormone GS1 and GR were added sequentially to a two-fold, three-fold, or four-fold dilution series of the test compounds to generate a competition curve. The test compounds we chose as controls were dexamethasone, cortisol and testosterone. For each well, 25 μL of 4×GS1 was added into 50 μL of the test compound, and was mixed by shaking on a plate shaker. 25 μL of 4x GR was then added and mixed well. The negative control was a well containing 50 μL Complete GR Screening Buffer, 25 μL 4x GS1 and 4x GR, where the positive control was identical to the negative control, but included 1mM dexamethasone, representing 100% competition. A well with only GR was used as a blank control. The plate was incubated at 4 °C in the dark for 4 h, 8 h and 16 h as well as at 20 °C (room temperature) in the dark to 2 h, 3 h and 4 h. A plate reader was employed to measure the fluorescence polarization value of each well. The cell pellets and supernatants from both cultures were assayed at 2 times and 10 times dilution. Different conditions of control assays were run in parallel to adjust the results.

Chapter 3. Results and Discussion

3.1. LDL composition

3.1.1. LDL collection

Complete purification of LDL was achieved by dialysis of plasma supernatant treated with ammonium sulfate. Dialysis made the LDL molecules clump together and, due to their low density, float after being centrifuged. After lyophilization, we successfully obtained 1500 mg pure LDL from 15 eggs, which corresponded to 200 ml egg yolk.

TLC analysis of the floating residue, which was LDL, demonstrated that there were two major compounds: cholesterol ester and cholesterol. The SDS-PAGE pattern showed that LDL consists of five major apoproteins with molecular weights of about 15, 60, 65, 80 and 140 kilo Dalton (kDa) (Figure 3-1). The bands around 40 kDa, which were also concentrated, were the result of contamination by β-livetin. Thus, the composition matched what was reported in the literature.

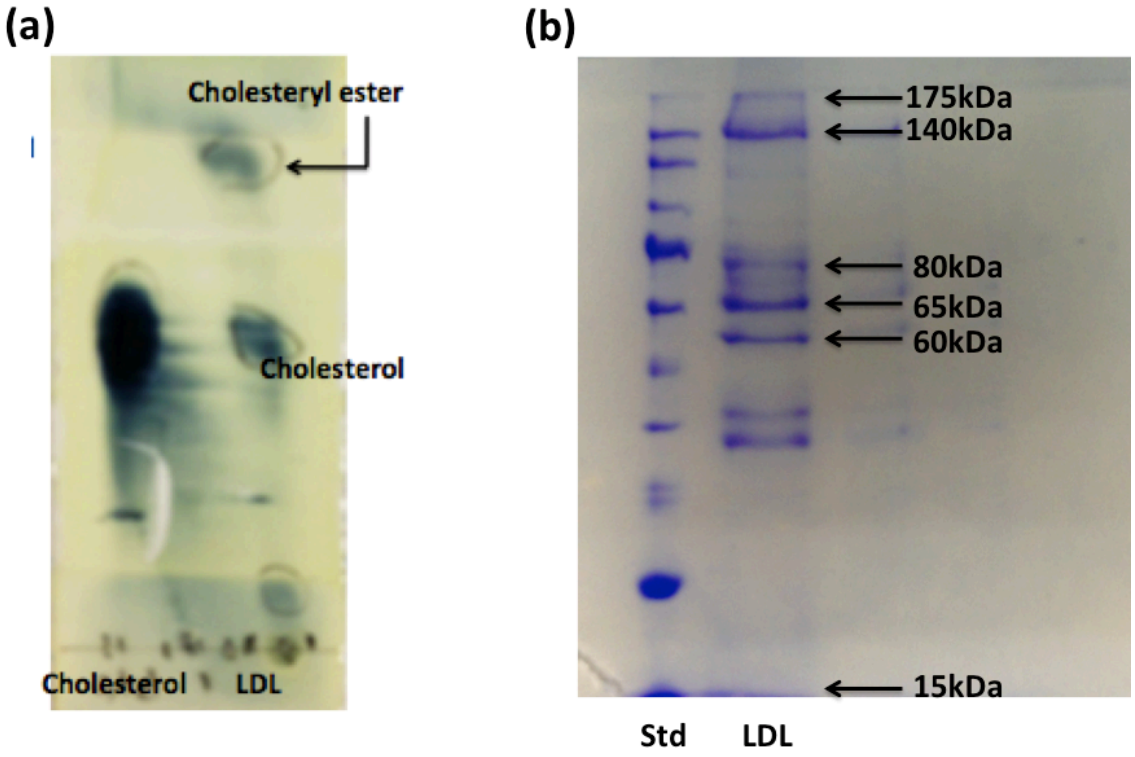

Figure 3-1. TLC and SDS-PAGE GEL of LDL-cholesterol. (a) TLC analysis with cholesterol as a standard indicated there were two major compounds: cholesterol ester and cholesterol; (b) Protein analysis of LDL-cholesterol by SDS-PAGE indicated five major apoproteins.

3.1.2. Total cholesterol oxidation assay

In order to determine the amount of free cholesterol and total cholesterol in LDL, a total cholesterol assay were set up.

Standard curves of cholesterol oxidation were first tried at 240 nm. The concentration of free cholesterol in LDL was measured by applying the standard curve. LDL contains less than 1% free cholesterol by weight. In order to determine the total cholesterol (free and esterified) in LDL, we incubated LDL with esterase for 30 minutes before adding cholesterol oxidase. The results were either too low to fit in the accurate range or too turbid to be detected accurately by

UV-Vis at 240 nm because of the white precipitation when we tried to increase the concentration of LDL.

In order to solve the problem at 240 nm and to measure the absorbance accurately, the total cholesterol assay was set up. Following the reaction of 4-aminoantipyrine, hydrogen peroxide, and phenol, catalyzed by MRP, quinoneimine dye with red color accumulated. The dye has an absorbance at 505 nm. With more accurate and repeatable results, the standard curve of absorbance relative to concentrations of free cholesterol was obtained (Figure 3-2). The concentration of free cholesterol in LDL was measured by fitting the values of absorbance into the standard curve. The results we got at 505 nm repeated the results at 240 nm, which indicating the results were reliable and reproducible

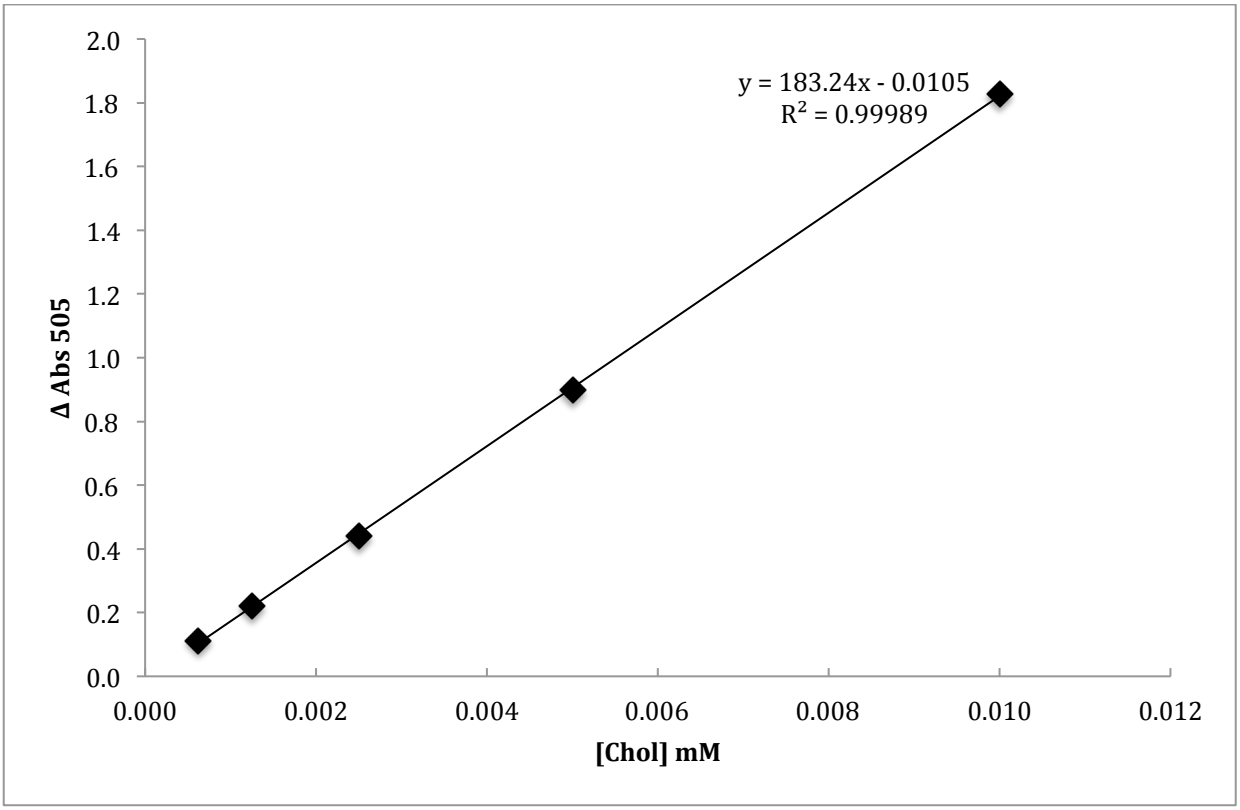

Figure 3-2. Standard curve for cholesterol oxidation assay II. The standard curve was obtained by measuring the change in UV absorbance at 505 nm (ΔAbs_{505}), which is caused by the formation of quinoneimine dye. ΔAbs_{505} is plotted verse concentration of cholesterol which ranged from 0.0006 mM to 0.01 mM.

After confirming that the MRP-coupled cholesterol oxidation assay worked reliably, the cholesterol esterase assay was implemented to set up the total cholesterol assay. In order to obtain a standard curve, different volumes of cholesteryl acetate (4.4 mg/mL in isopropanol) were incubated with oxidase (0.68 μM, 2 μL) and peroxidase (8200 n/mL, 3 μL) in master batch (0.1M Phosphate buffer, pH=7.0, 0.7 mM 4-aminoantipyrine, 5.0 nM phenol, 0.4 mM sodium cholate) for 10 minutes. After adding esterase (8.44 mg/mL, 50 μL), which is responsible for transforming of cholesteryl acetate into cholesterol, the following oxidation and peroxidation reaction would happen in turn, producing quinoneimine dye. The appearance of quinoneimine dye lead to the changes of absorbance at 505 nm by UV-vis. The data was plotted verse

concentration (Figure 3-3). In this way, the final concentration of total cholesterol in LDL was successfully measured to be 50% by weight.

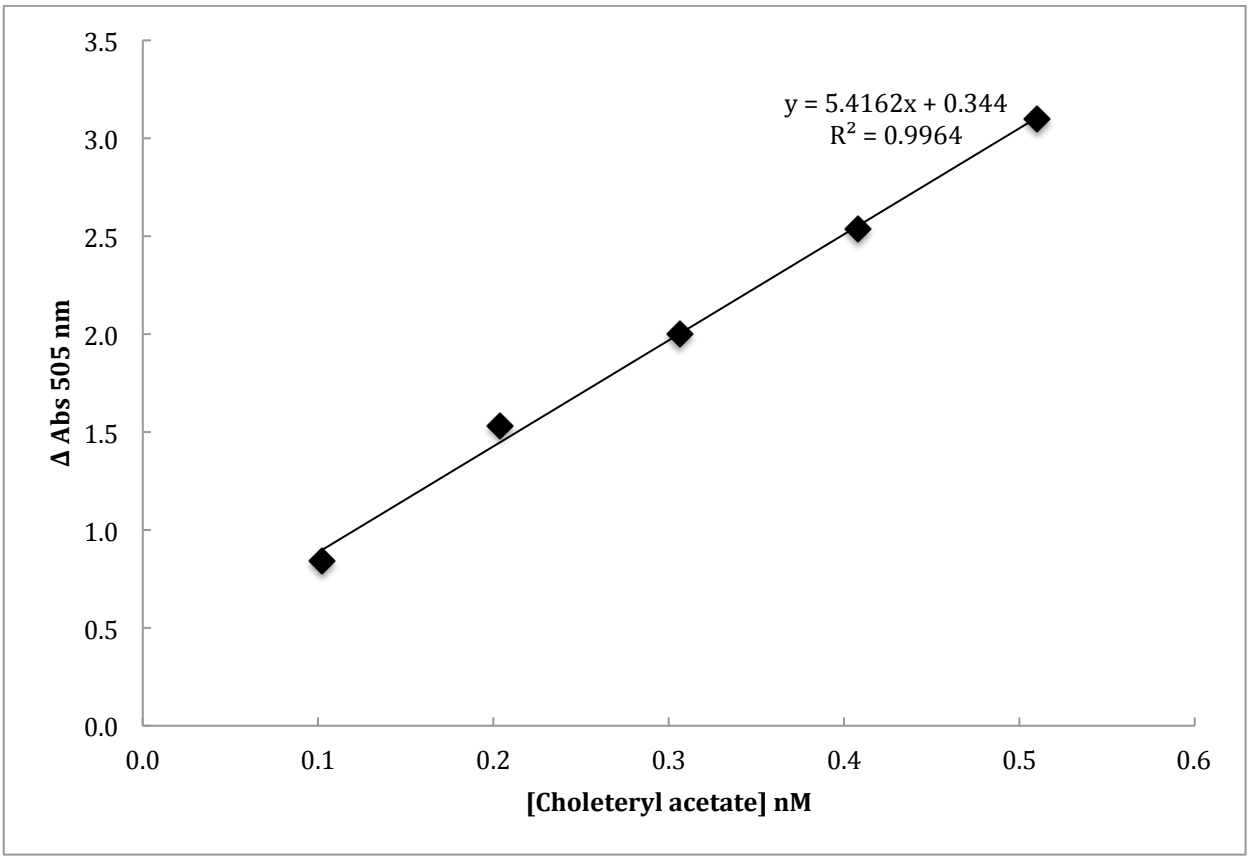

Figure 3-3. Standard curve for total cholesterol assay at 505 nm. The standard curve was obtained by measuring the change in UV absorbance at 505 nm (ΔAbs_{505}), which is caused by the formation of quinoneimine dye. ΔAbs_{505} are plotted verse concentration of cholesteryl acetate, which ranged from 0.1 mM to 0.5 mM. (0.1M Phosphate buffer, pH=7.0, 0.7 mM 4-aminoantipyrine, 5.0 nM phenol, 0.4 mM sodium cholate)

3.1.3. Growth of *M. smegmatis* and lipid extraction

M. smegmatis was successfully grown on both 7H9 liquid media as well as 7H10 solid media with either glycerol or LDL-cholesterol. During the experiments, we found that *M. smegmatis* grew much slower on LDL-cholesterol than on glycerol. We also proved that by

scaling up the volumes of the culture step by step, starting from 2 mL total volume, then diluting 1 mL from the culture into 10 mL, followed by 10 mL into 100 mL, and up to 250 mL, reduces contamination and shortens the culture growth process.

Following the supernatant (ethyl acetate extraction) and cell pellets (Bligh-Dyer method) extraction method, we obtained residues of both supernatant extracts and cell pellets extracts. The extracts were weighted and dissolved in DMSO for following study.

3.2. Glucocorticoid receptor competitor assay

3.2.1. Standard

The concentration of the test compound that results in a half-maximal shift in polarization value is the IC_{50} for the compounds. Based on this measurement, the relative affinity of the test compounds for GR can be measured.

Before running the assay against cell pellet and culture supernatant from *M. smegmatis*, several candidate hormone compounds, including dexamethasone, cortisol and testosterone, were assayed to make a standard curve as well as to test whether the assay can work well and is repeatable.

After several trials, dexamethasone, with most ideal value of IC_{50}, was chosen to fit a standard curve for the study of the relative affinities of the candidate compounds from cell supernatant (Figure 3-4).

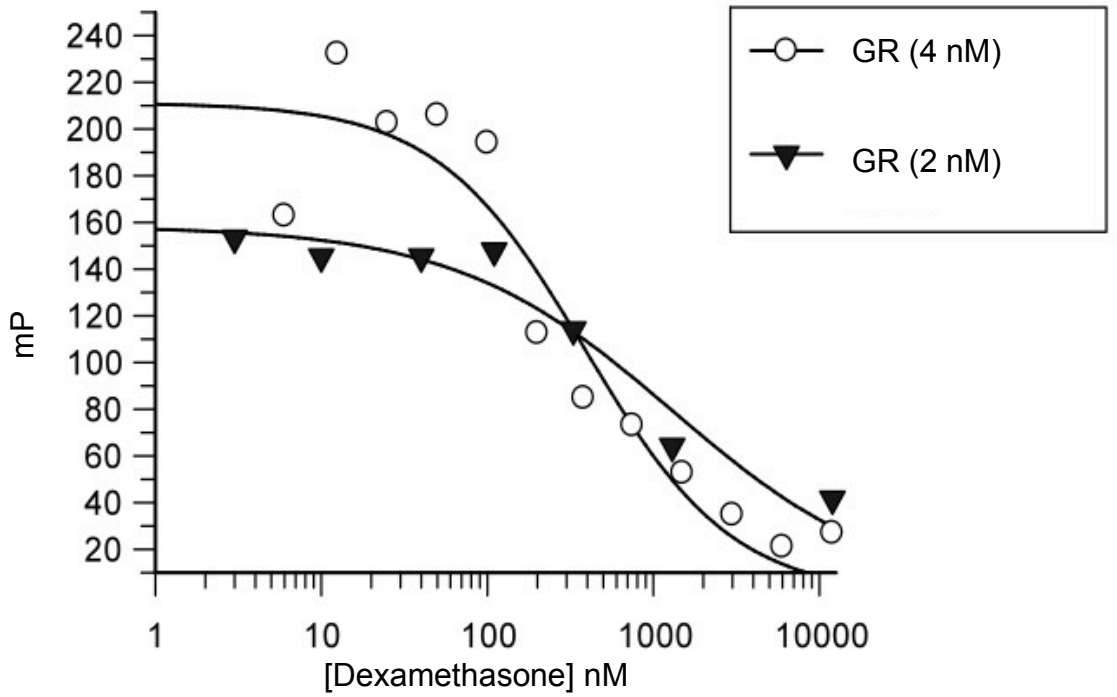

Figure 3-4. Standard FP assay with dexamethasone. The fluorescence polarization value drops with increasing dexamethasone concentration indicating dexamethasone can displace the fluorophore GS1 from the glucocorticoid receptor (GR). Empty circles represent [GR]= 4 nM, while solid triangles represent [GR]= 2 nM with [GS1]= 2.5 nM.

3.2.2. GR assays screening for candidate hormone compounds

Repeatable results for the glucocorticoid receptor assay using dexamethasone as a standard demonstrate that the assay can detect the steroid compound efficiently. This means it is a good method for the further study of screening for candidate hormone compounds from the supernatant or pellets from the cells of *M. smegmatis* grown either on glycerol or LDL-cholesterol. Based on the mechanism of *M. tuberculosis'* s infection and on previous *M.*

tuberculosis metabolism studies, both, *in vitro* and *in vivo*, our hypothesis is as follows: 1) No competitive compounds are expected in either cell pellets or supernatant from *M. smegmatis* grown on glycerol; 2) No competitive compounds are expected in cell pellets from *M. smegmatis* grown on LDL-cholesterol; 3) Competitive compounds from culture supernatant of the glucocorticoid receptor are expected to be identified by screening fluorescence polarization and by observing a drop in mP values.

Cell pellets

As a negative control, the GR assay was run against cell pellets from *M. smegmatis* that was grown on, either, glycerol or LDL-cholesterol. Pellet extract samples were first screened under the same condition used for the standard assay. First, we studied cell pellets from *M. smegmatis* grown on glycerol. The pellet extracts were resuspended in DMSO to make a stock sample. The stock sample (4.6 μL) was diluted into 95.4 μL assay working buffer for the FP assay, and, starting from 32000 μg/ml, was serially diluted with working buffer (100 μL) containing 4.6% DMSO into each well. The FP values remained consistently high indicating that no displacement occurred, which confirmed the hypothesis that no competitive could be found in cell pellets (Figure 3-5).

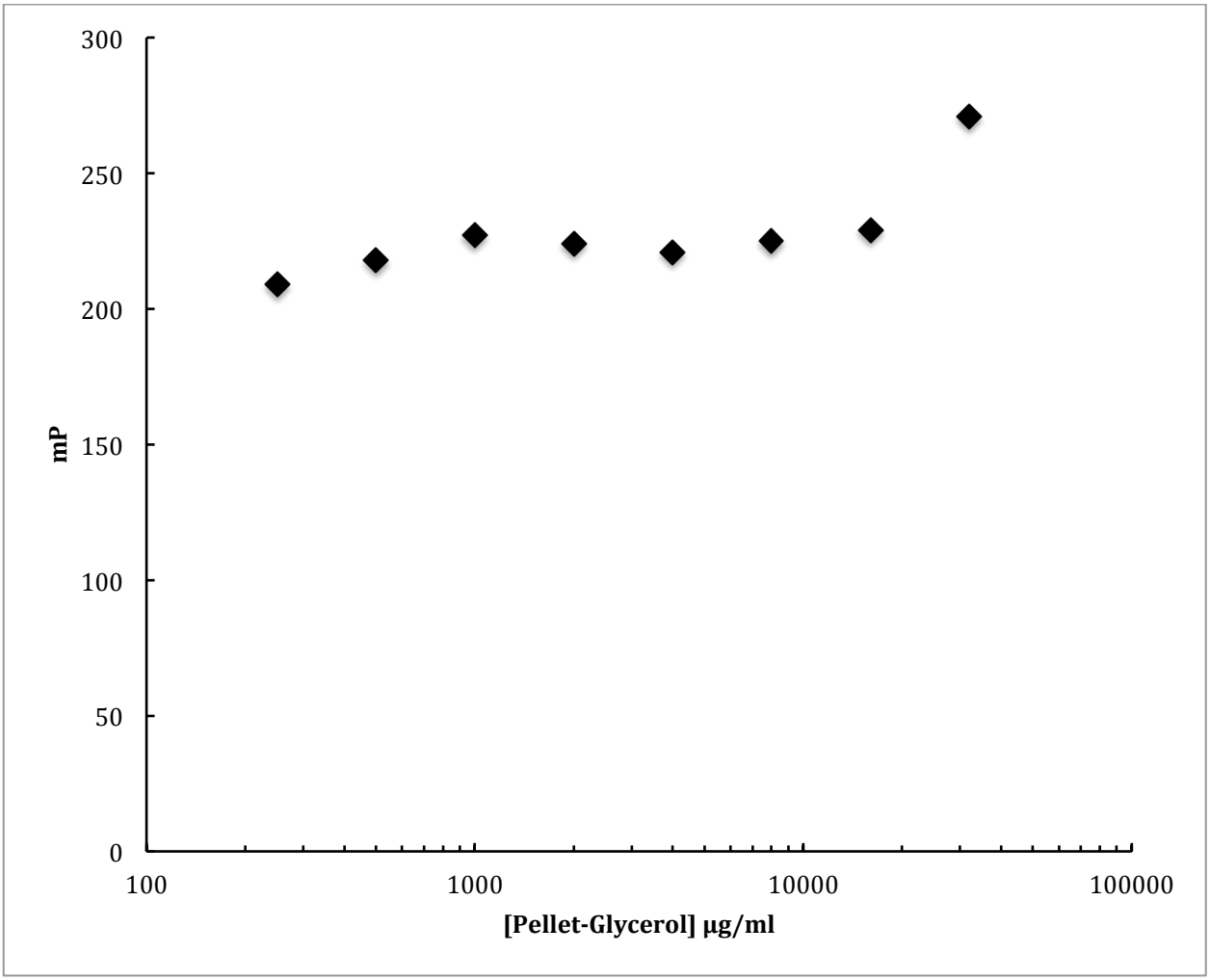

Figure 3-5. FP assay against cell pellets from *M. smegmatis* grown on glycerol. Cell pellets extracts were concentrated, and the residues were resuspended in DMSO and diluted with FP assay working buffer (final [DMSO] maintained at 4.6% v/v). 25 µL serially diluted samples, starting from 3200 µg/mL, were added into each well with working buffer, GR, and GS1 compound (100 µL in total). The FP values remained consistently high indicating no competitive compound displaced GS1 from GR.

We ran FP assays to determine if GR ligands were present in cell pellets from *M. smegmatis* grown on LDL-cholesterol. Within the tested concentration range (starting from 1000 µg/mL to 7.5 µg/mL), competitive compounds were not found (Figure 3-6).

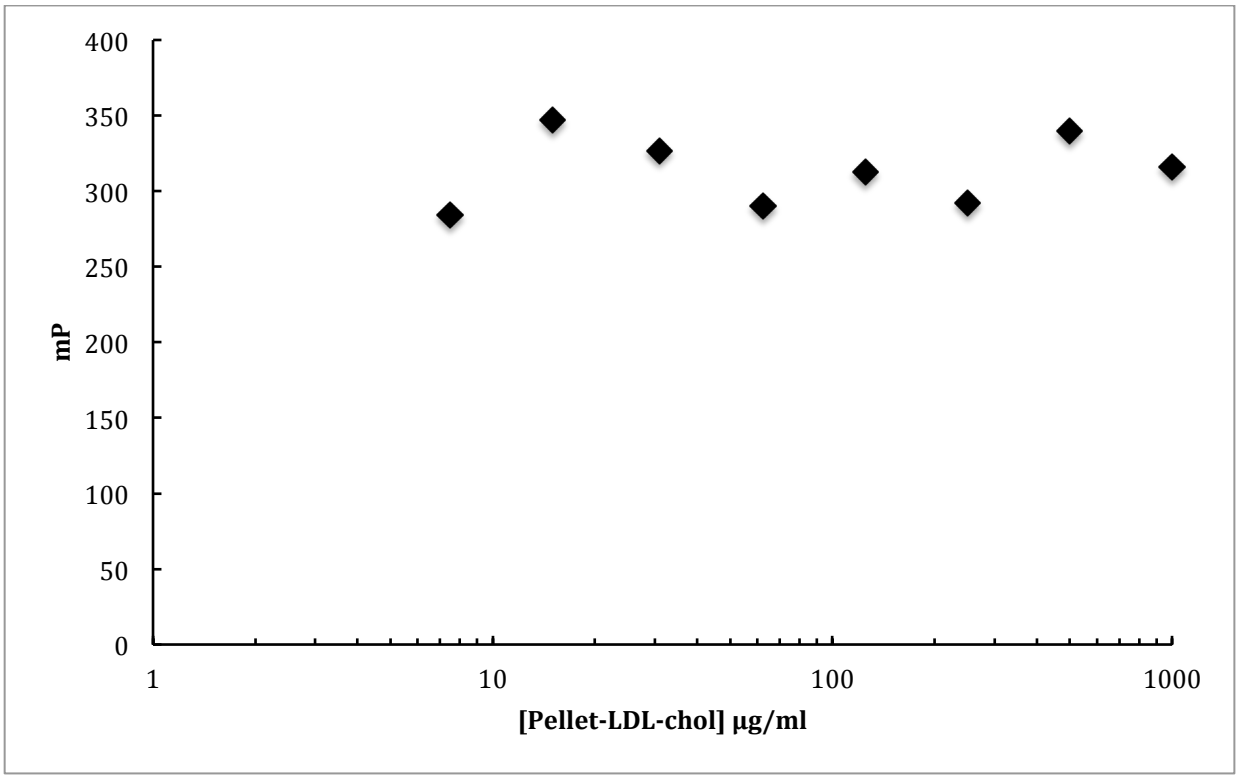

Figure 3-6. FP assay against cell pellets from *M. smegmatis* grown on LDL-cholesterol. Cell pellets extracts were concentrated, and the residues were resuspended in DMSO and diluted with FP assay working buffer (final [DMSO] maintained at 4.6% v/v). 25 µL serially diluted samples, starting from 1000 µg/mL, were added into each well with working buffer, GR, and GS1 compound (100 µL in total). The FP values remained consistently high indicating no competitive compound displaced GS1 from GR.

In cell pellets from *M. smegmatis* grown on, either, glycerol or LDL-cholesterol, we did not detect any competitive compound that could displace GS1 from GR, supporting our hypothesis that no competitive compound would be found in cell pellet extracts.

Cell supernatant

Different growth cultures and extract conditions were used to study *M. smegmatis* supernatants (Table 3-1). For the FP assay, extracts were resuspended in DMSO to make stock sample and diluted with assay working buffer. Sample preparation details are discussed below.

Table 3-1. The samples of cell supernatants were grown in two media, suspended with glycerol or LDL-cholesterol. Culture supernatants were extracted and resuspended in DMSO to make stock samples. Stock samples (4.6 μL) were diluted with working buffer (95.6 μL), followed by serial dilutions.

Sample	Growth cultures **7H10 agar plate**	Growth cultures **7H9 liquid**	Number of dilution folds	Further purification	Starting concentrations of assay samples in FP working buffer	Figure
I_a	Glycerol	Glycerol	2	✖	1600 μg/mL	3-7,8
I_b			10	✖	1600 μg/mL	3-9
II	Glycerol	LDL-chol	2	✖	3000 μg/mL	3-10
III			2	✖	6000 μg/mL	3-10
III_b			10	✖	6000 μg/mL	
III_c			2	Ethyl acetate	6000 μg/mL	3-11
III_d			2	Chloroform	6000 μg/mL	3-11
II_b			2	Methanol	3000 μg/mL	3-12

As a basic control for the FP assay against cell supernatant from *M. smegmatis*, we measured FP values of extracts from *M. smegmatis* grown on glycerol (Sample I_a) without adding GR or GS1. We observed high signal of fluorescence polarization (Figure 3-7). Possible reasons for observing high FP values are listed: particle precipitation resulting in light scattering, contaminates, or some molecules or lipids from the extracts has fluorescence. Later we measured the absorbance at 600 nm by UV-vis excluding the possibility that there was particle absorbing at 600 nm.

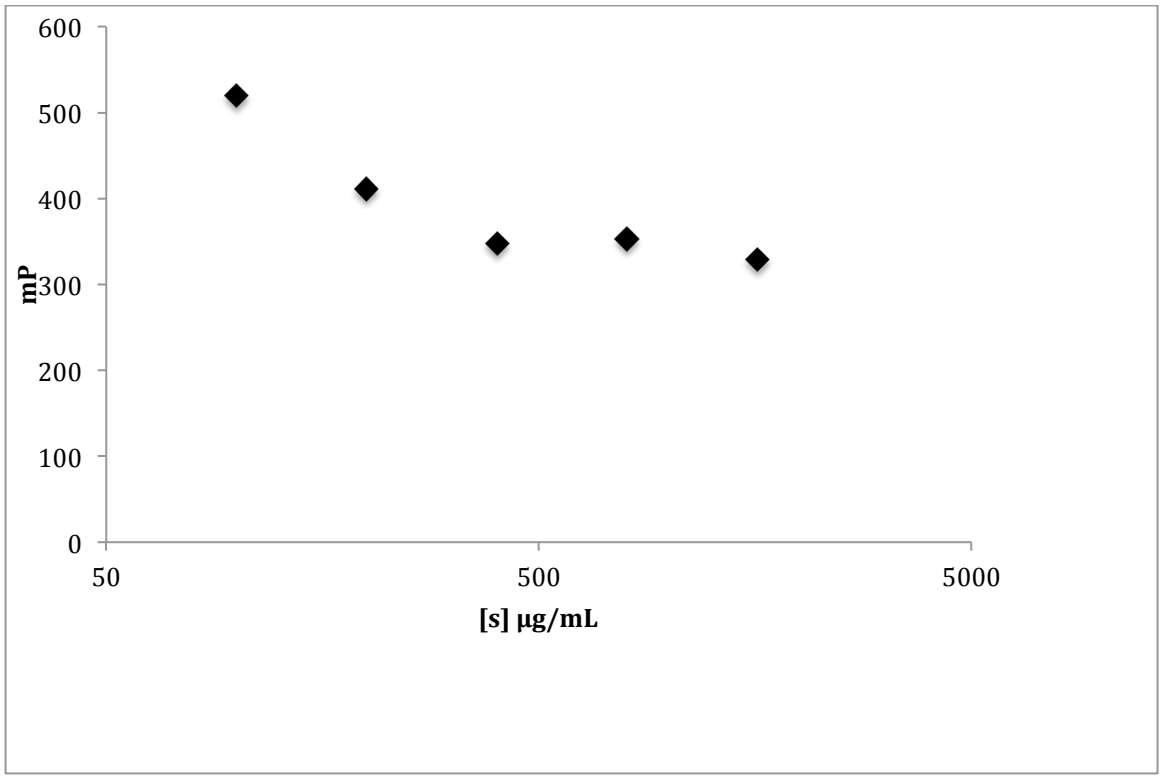

Figure 3-7. Fluorescence polarization of Sample I_a in the absence of GR and GS1. Supernatant of *M. smegmatis* cultures in 7H9 media supplemented with glycerol was extracted. The extracts were concentrated, and the residues were resuspended into DMSO and diluted with FP assay working buffer (final [DMSO] maintained at 4.6% v/v). 25 µL serially diluted samples, starting from 1600 µg/mL, were added into each well with 75 µL working buffer. The data indicated that there are some contaminates or fluorescent compounds influenced the results.

Next, we assayed Sample I_a with GR and GS1. The result was opposite to what was expected. The values of fluorescence polarization increased with increasing the concentration of extracts (Figure 3-8). The results were reproducible, excluding the possibility of an operational error.

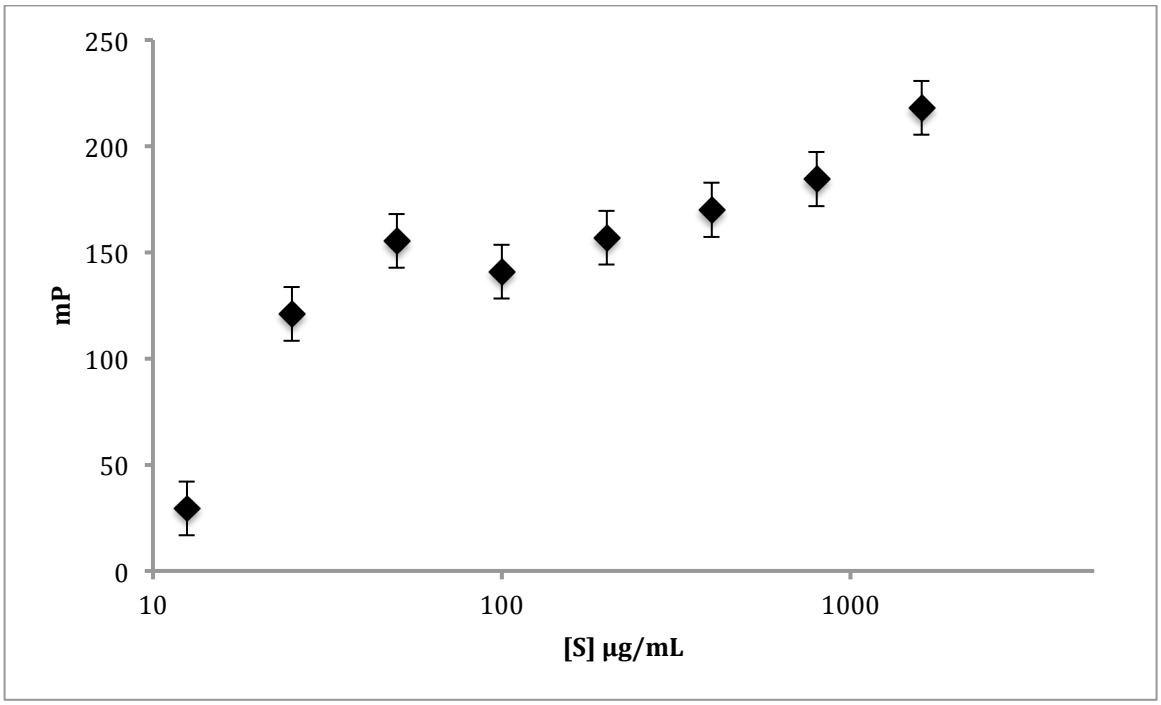

Figure 3-8. FP assay against Sample I_a. Supernatant of *M. smegmatis* cultures in 7H9 media supplemented with glycerol was extracted. The extracts were concentrated, and the residues were resuspended into DMSO and diluted with FP assay working buffer (final [DMSO] maintained at 4.6% v/v). 25 µL serially diluted samples, starting from 1600 µg/mL, were added into each well with working buffer, GR, and GS1 compound solutions (100 µL in total). FP values increased with the increase of the concentrations, and the results were reproducible.

Sample I_b, diluted from the same stock sample as Sample I_a, with five more times diluted, was tested using FP assay. The same trend was observed that fluorescence polarization increased with increasing the concentration of the extracts (Figure 3-9).

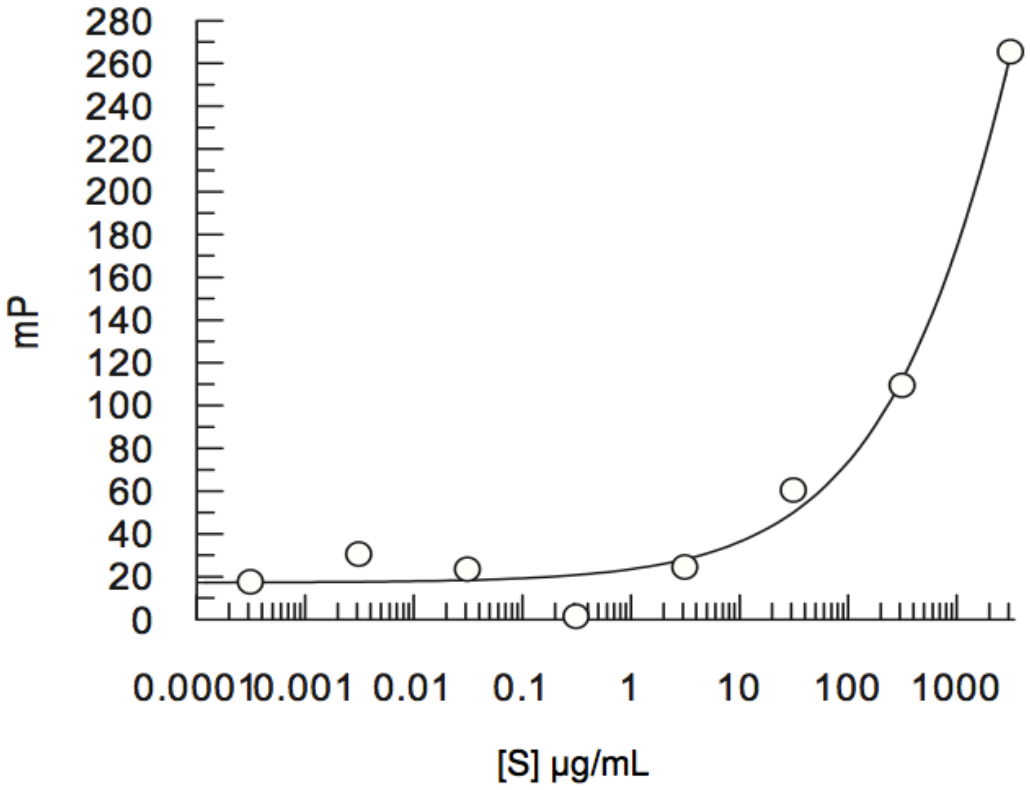

Figure 3-9. FP assay against Sample I_b. Supernatant of *M. smegmatis* cultures in 7H9 media supplemented with glycerol was extracted. The extracts were concentrated, and the residues were resuspended into DMSO and diluted with FP assay working buffer (final [DMSO] maintained at 4.6% v/v). 25 µL serially diluted samples, starting from 1600 µg/mL, were added into each well with working buffer, GR, and GS1 compound solutions (100 µL in total). FP values increased with increasing of supernatant extract concentrations.

Supernatant extracts from *M. smegmatis* grown on LDL-cholesterol were also screened under different conditions with FP assay. Our hypothesis was that *M. smegmatis,* which was induced by LDL-cholesterol, could metabolize competitive steroid compounds for the glucocorticoid receptor, which resulted in fluorescence polarization values dropping as the extract concentration increased. We first assayed the extracts grown on LDL-cholesterol (Sample II). Followed same procedures as Sample I, extracts were resuspended in DMSO to make a stock

sample of the extracts. The stock sample (4.6 µL) was diluted into 95.4 µL assay working buffer for the FP assay (3000 µg/mL). In order to exclude operational error, replicate assays were run (Sample III). Sample III was cultured in identical conditions with Sample II. The results showed same pattern with Sample I, which fluorescence polarization increased as the concentrations increased (Figure 3-10).

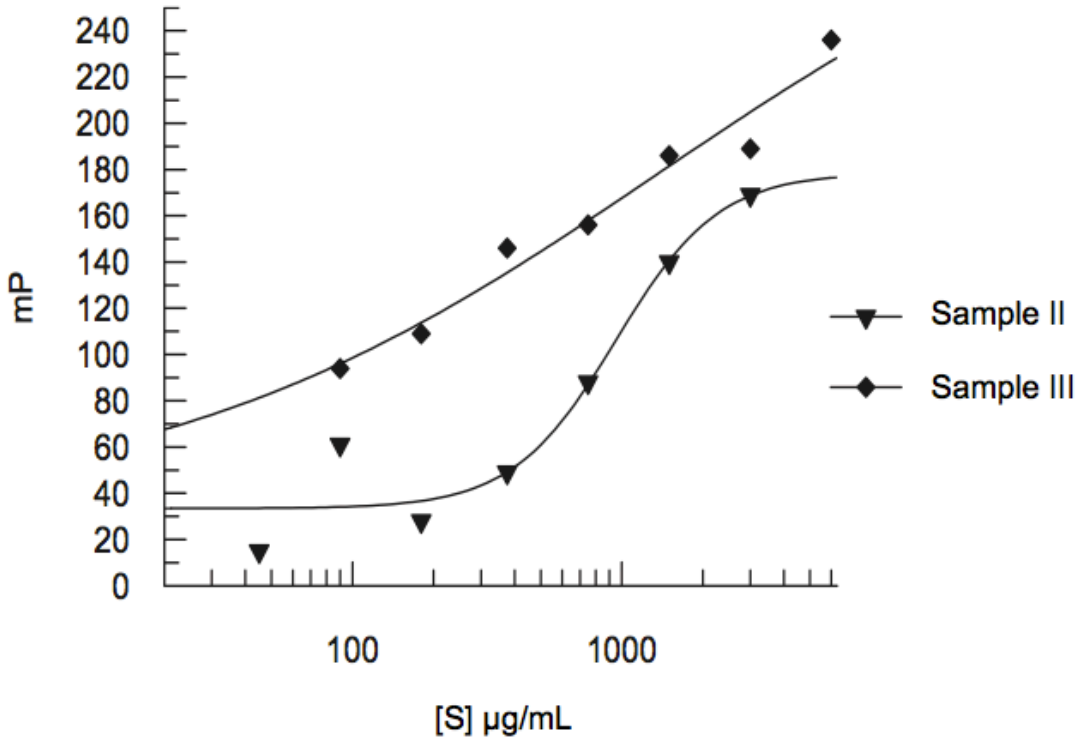

Figure 3-10. FP assay against Sample II and sample III. Supernatant of *M. smegmatis* cultures in 7H9 media supplemented with LDL-cholesterol was extracted. The extracts were concentrated and the residues were suspended in DMSO, and diluted with FP assay working buffer. (final [DMSO] maintained at 4.6% v/v). 25 µL serially diluted samples, starting from 3000 µg/mL (Sample II) or 6000 µg/mL (Sample III), were added into each well with working buffer, GR, and GS1 compound (100 µL in total). Sample II and sample III represent identical *M. smegmatis* cultures indicating the trends are reproducible.

We also expended the range of the concentrations of Sample III to analyze the trend of FP values. Sample III_b (6000 μg/mL) was diluted in 10-fold for each well and assayed against the FP assay. The result had the same trend as Sample III and Sample II (Table 3-2).

Table 3-2. FP assay against Sample III_b. Supernatant of *M. smegmatis* cultures in 7H9 media supplemented with LDL-cholesterol was extracted. The extracts were concentrated and the residues were suspended in DMSO, and diluted with FP assay working buffer (final [DMSO] maintained at 4.6% v/v). 25 μL serially diluted samples, starting from 6000 μg/mL, were added into each well with working buffer, GR, and GS1 compound (100 μL in total). The trend remained the same as Sample II and Sample III conforming to the trend in Figure 3-10.

[S] μg/ml	6000	600	60	6	0.6	0.06
mP	255	182	86	89	94	88

Based on the assumption that detergence might affect the fluorescent signal, we studied the assay against extracts of 7H9 media only supplemented with either glycerol or LDL-cholesterol. These two control assays were prepared identically with other assays against Sample I and Sample III with absence of *M. smegmatis* cells. Fluorescence polarization values remained consistently high, indicating there were no competitive compounds in the samples, excluding the possibility of influence of culture media.

Furthermore, we studied the possible influence of different solvent's solubility on supernatant extracts. We further purified Sample III by resuspending them in ethyl acetate (Sample III_c) or chloroform ($CHCl_3$) (Sample III_d), and concentrated them. The purified residues were resuspended in DMSO to make stock samples. Diluted by assay working buffer. The results of the two samples were plotted with the result for Sample III, indicating that all of them shared same pattern (Figure 3-11).

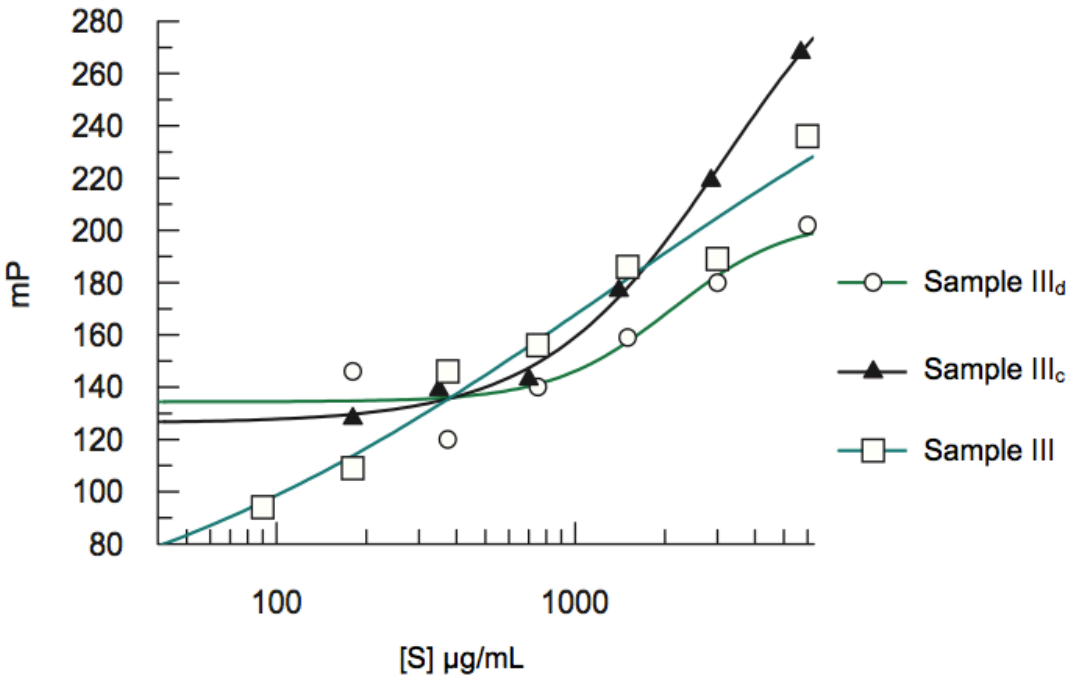

Figure 3-11. FP assay against Sample III, Sample III$_c$, and Sample III$_d$. Supernatant of *M. smegmatis* cultures in 7H9 media supplemented with LDL-cholesterol was extracted. The extracts were concentrated and further purified with EA or chloroform. The residues were suspended in DMSO, and diluted with FP assay working buffer (final [DMSO] maintained at 4.6% v/v). 25 µL serially diluted samples, starting from 6000 µg/mL, added into each well with working buffer, GR, and GS1 compound (100 µL in total). No significant differences were observed from the three samples.

According to the protocol of FP assay, methanol could also be used to make stock samples and assay samples. Followed by further purification with methanol and being concentrated, the residues (Sample II$_b$) were dissolved in either DMSO or methanol to prepare stock samples. The stock sample (4.6 µL) was added into 95.4 µL assay working buffer for FP assay (3000 µg/mL). Serial dilutions of the assay samples were added into each cell for the assay (Table 3-3). The fluorescence polarization values of Sample II$_b$ dissolved in methanol remained consistently high, while the value of Sample II$_b$ in DMSO showed an increase with the concentration increased (Figure 3-12).

Table 3-3. FP Assay against Sample II_b. Supernatant of *M. smegmatis* cultures in 7H9 media supplemented with LDL-cholesterol was extracted. The extracts were concentrated, and resuspended in methanol for further purification making it Sample II_b. Sample II_b was then concentrated again and was resuspended in either methanol or DMSO to prepare assay sample (final [DMSO] or [methanol] maintained at 4.6% v/v). 25 µL serially diluted samples, starting from 3000 µg/mL, added into each well with working buffer, GR, and GS1 compound (100 µL in total).

[Ex] µg/ml	3000	1500	750	375	180	90	45	22.5
mP(methanol)	284	290	274	251	233	172	210	179
mP(DMSO)	232	210	230	179	210	179	136	70

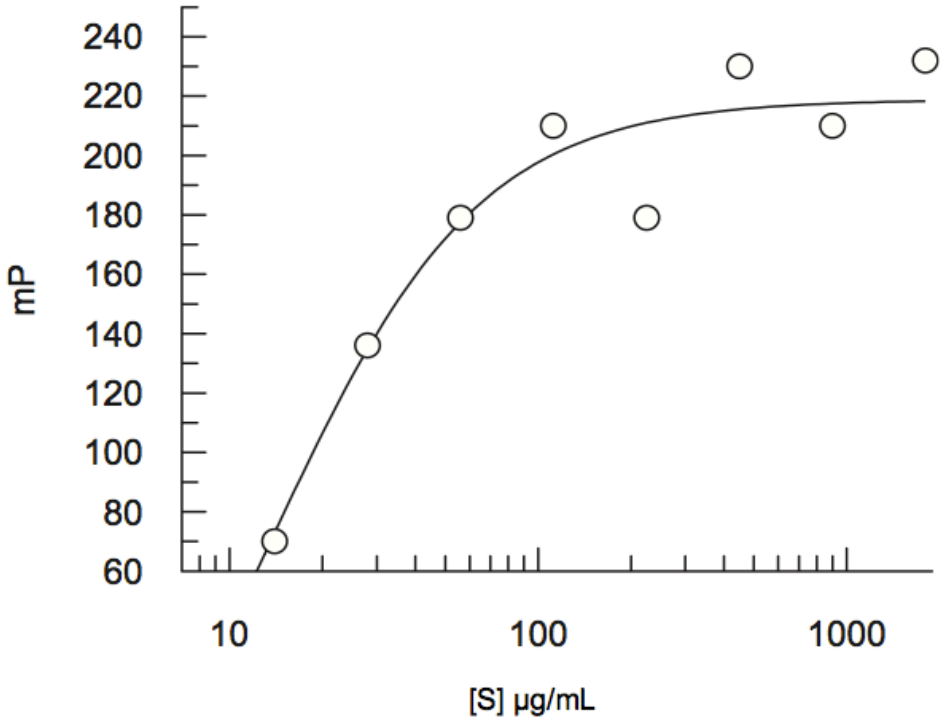

Figure 3-12. FP assay against Sample II_b. Supernatant of *M. smegmatis* cultures in 7H9 media supplemented with LDL-cholesterol was extracted. The extracts were concentrated, and resuspended in methanol for further purification (Sample II_b). Sample II_b was then concentrated again and was resuspended in DMSO to prepare assay sample (final [DMSO] maintained at 4.6% v/v). 25 µL serially diluted samples, starting from 3000 µg/mL, added into each well with working buffer, GR, and GS1 compound (100 µL in total). The results showed the same trend as Sample II_b

We ran LC/MS to separate the samples and studied the fractions. We ran the LC with water/methanol for 10 minutes, collected one-minute fractions and assayed the 10 samples. However, the signals were too low to analyze. In order to increase the concentration, we pooled triplicate samples. The fractions were resuspended in DMSO to make stock sample, two wells gave fluorescence polarization values around 150 mP, while other wells' results were all around 60 mP. The result indicated that there might be some compounds from supernatant of *M. smegmatis* supplemented with LDL-cholesterol could displace GS1 from GR, which could be chosen as the potential target for further study.

3.3. Conclusion and future directions

In our project, we successfully purified LDL-cholesterol from egg yolk with yield of 1500 mg out of 200 mL egg yolk. TLC analysis and protein composition analysis showed identical result of what have been reported from previous study, indicating the LDL complex was purified properly. After several trials, we set up an ideal total cholesterol assay for measuring the concentration of cholesterol from LDL. By measuring the absorbance at 505 nm by UV spectrum, the total concentration of cholesterol in LDL complex was determined as around 50% by weight. Dexamethasone, a well-known competitive compound against GR, was used as standard to set up the glucocorticoid receptor competitor assay.

In our studies, no competitive compounds were found in cell pellets from *M. smegmatis* grown on either glycerol or cholesterol. Being fractionated by LC and analyzed by the assay, the sample showed low fluorescence polarization value, indicating displacement of GS1 from GR

happened. From then, we concluded that cell supernatant from *M. smegmatis* grown on cholesterol might have competitive compounds against glucocorticoid receptor, which could be candidate immunomodulators.

However, identification and determination of the existence of competitive compounds against glucocorticoid receptor have not been fully established. The results of assays against cell supernatant of *M. smegmatis* shared the same pattern that fluorescence polarization value increased with the increase of concentration of the extracts, which were opposite to what we were expected. The results indicated there were some complex from the cells themslves influencing the results. We already excluded the possibility of scattering at 600 nm by UV spectrum. In order to further study the supernatant extracts, size exclusion is needed to identify whether there are lipids or forming of micelles. Also, since fluorescence polarization is a kind of assay format only binding-affinity related, activity-based protein profiling could be considered as a complementary method. After determining the existence of competitive compounds, we plan to fractionate the extracts to isolate the active components and determine their molecular identity.

Reference

1. World Health Organization, Fact Sheets on tuberculosis No. 104. **2007**.
2. World Health Organization. Global tuberculosis control 2011.
3. Rahman, S., B. Gudetta, J. Fink, A. Granath, S. Ashenafi, A. Aseffa, M. Derbew, M. Svensson, J. Andersson and S. G. Brighenti, Compartmentalization of immune responses in human tuberculosis: few CD8+ effector T cells but elevated levels of FoxP3+ regulatory T cells in the granulomatous lesions. *Am. J. Pathol.* **2009,** *174*, 2211-2224.
4. Donoghue, H. D.; Spigelman, M.; Greenblatt, C. L.; Lev-Maor, G.; Bar-Gal, G. K.; Matheson, C.; Vernon, K.; Nerlich, A. G.; Zink, A. R., Tuberculosis: from prehistory to Robert Koch, as revealed by ancient DNA. *Lancet Infect. Dis.* **2004,** *4* (9), 584-592.
5. Scheindlin, S., The fight against tuberculosis. *Mol. Interventions* **2006,** *6* (3), 124-130.
6. Kaufmann Stefan, H. E., Robert Koch, the Nobel Prize, and the ongoing threat of tuberculosis. *N Engl J Med* **2005,** *353* (23), 2423-6.
7. Madkour, M. M., *Textbook of tuberculosis*. Springer: New York, 2003.
8. Ryan, K. J.; Sherris, J. C., *Sherris medical microbiology*. 3rd ed.; Appleton & Lange: Norwalk, Conn., 1994; p xiii, 890 p.
9. Russell, D. G.; Barry, C. E., 3rd; Flynn, J. L., Tuberculosis: what we don't know can, and does, hurt us. *Science* **2010,** *328* (5980), 852-6.
10. Peyron, P.; Vaubourgeix, J.; Poquet, Y.; Levillain, F.; Botanch, C.; Bardou, F.; Daffe, M.; Emile, J. F.; Marchou, B.; Cardona, P. J.; de Chastellier, C.; Altare, F., Foamy macrophages from tuberculous patients' granulomas constitute a nutrient-rich reservoir for M. tuberculosis persistence. *PLoS Pathog* **2008,** *4* (11), e1000204.
11. Clemens, D. L., Characterization of the Mycobacterium tuberculosis phagosome. *Trends in Microbiology* **1996,** *4* (3), 113-118.
12. Rohde, K. Yates, R. M. Purdy, G. E. Russell, D. G., Mycobacterium tuberculosis and the environment within the phagosome. *Immunological Reviews* **2007,** *219*, 37-54.
13. Mann, F. M., M. Xu, X. Chen, D. B. Fulton, D. G. Russell and R. J. Peters Edaxadience: a new bioactive diterpene from Mycobacterium tuberculosis. *J. Am. Chem. Soc* **2009,** *131*, 17526-17527.
14. Winau, F.; Weber, S.; Sad, S.; de Diego, J.; Hoops, S. L.; Breiden, B.; Sandhoff, K.; Brinkmann, V.; Kaufmann, S. H.; Schaible, U. E., Apoptotic vesicles crossprime CD8 T cells and protect against tuberculosis. *Immunity* **2006,** *24* (1), 105-17.
15. Pandey, A. K.; Sassetti, C. M., Mycobacterial persistence requires the utilization of host cholesterol. *Proc Natl Acad Sci* **2008,** *105* (11), 4376-80.
16. Puissegur MP; Lay G; Gilleron M; Botella L; Nigou J; Marrakchi H; Mari B; Duteyrat JL; Gueradel Y; Kremer L; Barbry P; Puzo G; F., A., Mycobacterial lipomannan induces granuloma macrophage fusion via a TLR2-dependent, ADAM9- and beta 1integrin-mediated pathway. *J Immunol.* **2007,** *178* (5), 3161-9.
17. Vogt, G.; Nathan, C., In vitro differentiation of human macrophages with enhanced antimycobacterial activity. *Journal of Clinical Investigation* **2011,** *121* (10), 3889-3901.
18. (a) Byarugaba, D. K., Antimicrobial resistance in developing countries and responsible risk factors. *Int. J. Antimicrob. Agents* **2004,** *24* (2), 105-110;
    (b) Mwinga, A.; Bernard Fourie, P., Prospects for new tuberculosis treatment in Africa. *Trop Med Int Health* **2004,** *9* (7), 827-32.

19. (a) Raviglione, M. C.; Smith, I. M., XDR tuberculosis--implications for global public health. *N Engl J Med* **2007,** *356* (7), 656-9;
(b) Mandavilli, A., Virtually incurable TB warns of impending disaster. *Nat Med* **2007,** *13* (3), 271.
20. (a) World Health Organization, MDR and XDR-TB progress report. **2011**;
(b) World Health Organization, Tuberculosis facts. **2009**.
21. (a) Kochi, A., The global tuberculosis situation and the new control strategy of the World Health Organization. *Tubercle* **1991,** *72* (1), 1-6;
(b) Rattan, A.; Kalia, A.; Ahmad, N., Multidrug-resistant *Mycobacterium tuberculosis*: molecular perspectives. *Emerg Infect Dis* **1998,** *4* (2), 195-209.
22. World Health Organization. *HIV and TB (TB/HIV) - fact sheet*; 2011.
23. Gupta, P.; Jadaun, G. P.; Das, R.; Gupta, U. D.; Srivastava, K.; Chauhan, A.; Sharma, V. D.; Chauhan, D. S.; Katoch, V. M., Simultaneous ethambutol & isoniazid resistance in clinical isolates of Mycobacterium tuberculosis. *Indian J Med Res* **2006,** *123* (2), 125-30.
24. Pucci, M. J.; Bronson, J. J.; Barrett, J. F.; DenBleyker, K. L.; Discotto, L. F.; Fung-Tomc, J. C.; Ueda, Y., Antimicrobial evaluation of nocathiacins, a thiazole peptide class of antibiotics. *Antimicrob Agents Chemother* **2004,** *48* (10), 3697-701.
25. Reddy, V. M.; O'Sullivan, J. F.; Gangadharam, P. R., Antimycobacterial activities of riminophenazines. *J Antimicrob Chemother* **1999,** *43* (5), 615-23.
26. Huebner, R. E.; Castro, K. G., The changing face of tuberculosis. *Annu Rev Med* **1995,** *46*, 47-55.
27. Brzostek, A.; Sliwinski, T.; Rumijowska-Galewicz, A.; Korycka-Machala, M.; Dziadek, J., Identification and targeted disruption of the gene encoding the main 3-ketosteroid dehydrogenase in Mycobacterium smegmatis. *Microbiology* **2005,** *151* (Pt 7), 2393-402.
28. McKinney, J. D., et al., Persistence of Mycobacterium tuberculosis in marcrophages and mice requires the glyoxylate shunt enzyme isocitrate lyase. *Nature* **2000,** *406*, 735-738.
29. Cole, S. T., Brosch, R., et al., Deciphering the biology of Nycobacterium tuberculosis from the complete genome sequence. *Nature* **1998,** *393*, 537-544.
30. (a) Maxfield, F. R.; Wustner, D., Intracellular cholesterol transport. *J Clin Invest* **2002,** *110* (7), 891-8;
(b) Wustner, D.; Mondal, M.; Tabas, I.; Maxfield, F. R., Direct observation of rapid internalization and intracellular transport of sterol by macrophage foam cells. *Traffic* **2005,** *6* (5), 396-412.
31. Schnappinger D; Ehrt S; Voskuil MI; Liu Y; Mangan JA; Monahan IM; Dolgannov G; Efron B; Butcher PD; Nathan C; GK, S., Transcriptional Adaptation of Mycobacterium tuberculosis within Macrophages: Insights into the Phagosomal Evironment. *J Exp Med.* **2003,** *198* (5), 693-704.
32. Mohn, W. W.; van der Geize, R.; Stewart, G. R.; Okamoto, S.; Liu, J.; Dijkhuizen, L.; Eltis, L. D., The actinobacterial mce4 locus encodes a steroid transporter. *J Biol Chem* **2008,** *283* (51), 35368-74.
33. Garton, N. J.; Waddell, S. J.; Sherratt, A. L.; Lee, S. M.; Smith, R. J.; Senner, C.; Hinds, J.; Rajakumar, K.; Adegbola, R. A.; Besra, G. S.; Butcher, P. D.; Barer, M. R., Cytological and transcript analyses reveal fat and lazy persister-like bacilli in tuberculous sputum. *PLoS Med* **2008,** *5* (4), e75.

34. Av-Gay, Y.; Sobouti, R., Cholesterol is accumulated by mycobacteria but its degradation is limited to non-pathogenic fast-growing mycobacteria. *Canadian Journal of Microbiology* **2000,** *46* (9), 826-831.
35. Nesbitt, N. Y., X.; Fontán, P.; Kolesnikova, I.; Smith, I.; Sampson, N. S.; Dubnau, E., A thiolase of M. tuberculosis is required for virulence and for production of androstenedione and androstadienedione from cholesterol. *Infect. Immun.* **2010,** *78* (1), 275-82.
36. Corrales, J. J., M. Alneida, R. Burgo, M. T. Mories, J. M. Miralles and O. A., Androgen-replacement therapy depresses the ex vivo production of inflammatory cytokines by circulating antigen-presenting cells in aging type-2 diabetic men with partial androgen deficiency. *J. Endocrin* **2006,** *189*, 595-604.
37. Kelley, K. W., Weigent, D.A. & Kooijman, R. , Protein hormones and immunity. *Brain, Behavior, and Immunity,* **2007,** *21*, 384-392.
38. Annice Mukherjee, M. H., Julian Davis and Stephen Shalet, Immune fuction in hypopituitarism: time to reconsider? *Clinical Endocrinology* **2010,** *73* (4), 425-431.
39. Sternberg, E. M., Neural regulation of innate immunity: a coordinated nonspecific host response to phathogens. *Nat Rev Immunol.* **2006,** *6*, 318-28.
40. Chocano-Bedoya, P.; Ronnenberg, A. G., Vitamin D and tuberculosis. *Nutrition Reviews* **2009,** *67* (5), 289-293.
41. Liu, P. T., S. Stenger, H. Li, L. Wenzel, B. H. Tan, S. R. krutzik, M. T. Ochoa, J. Schauber, K.wu, C. Meinken, D. L. Kamen, M. Wagner, R. Bals, A. Sternmeyer, U. Zugel, R. L. Galllo, D. Eisenberg, M. Heweson B.W. Hollis and R. L. Modin, Toll-like receptor triggering of a vitamin D-mediated human abtimicrobial response. *Science* **2006,** *311*, 1770-1773.
42. R. L. Modlin, G. C., *Nat. Med.* **2004,** *10*, 1173.
43. Tufariello, J. M., J. Chan and J. L. Flynn, Latent tuberculosis: mechanisms of host the bacillus that contribute to persistnet infection. *J. Immunol* **2003,** *176*, 578-590.
44. Martineau, A. R.; Wilkinson, R. J.; Wilkinson, K. A.; Newton, S. M.; Kampmann, B.; Hall, B. M.; Packe, G. E.; Davidson, R. N.; Eldridge, S. M.; Maunsell, Z. J.; Rainbow, S. J.; Berry, J. L.; Griffiths, C. J., A single dose of vitamin D enhances immunity to mycobacteria. *Am J Respir Crit Care Med* **2007,** *176* (2), 208-13.
45. Mangelsdorf, D. J.; Evans, R. M., The RXR heterodimers and orphan receptors. *Cell* **1995,** *83* (6), 841-50.
46. Bensinger, S. J.; Bradley, M. N.; Joseph, S. B.; Zelcer, N.; Janssen, E. M.; Hausner, M. A.; Shih, R.; Parks, J. S.; Edwards, P. A.; Jamieson, B. D.; Tontonoz, P., LXR signaling couples sterol metabolism to proliferation in the acquired immune response. *Cell* **2008,** *134* (1), 97-111.
47. Joseph, S. B.; Castrillo, A.; Laffitte, B. A.; Mangelsdorf, D. J.; Tontonoz, P., Reciprocal regulation of inflammation and lipid metabolism by liver X receptors. *Nat Med* **2003,** *9* (2), 213-9.
48. Castrillo A, J. S., Vaidya SA, Haberland M, Fogelman AM, Cheng G, Tontonoz P, Crosstalk between LXR and toll-like receptor signaling mediates bacterial and viral antagonism of cholesterol metabolism. *Mol Cell* **2003,** *12* (4), 805-16.
49. Chrousos GP, C. E., Kino T., The Glucocorticoid receptor gene, longevity, and the complex disorders of Western societies. *Am J Med* **2004,** *117*, 204-207.

50. (a) Chrousos, G. P., The glucocorticoid receptor gene, longevity, and the complex disorders of Western societies. *Am J Med* **2004,** *117* (3), 204-7;
(b) Kino, T.; Charmandari, E.; Chrousos, G. P., *Glucocorticoid action : basic and clinical implications*. New York Academy of Sciences: New York, 2004; p xi, 221 p.
51. (a) K., D. B., Selective Glucocorticoid Receptor modulators. *J Steroid Biochemistry Mol Biol* **2010,** *120* (2-3), 96-104;
(b) Papadimitriou, A.; Priftis, K. N., Regulation of the Hypothalamic-Pituitary-Adrenal Axis. *Neuroimmunomodulation* **2009,** *16* (5), 265-271.
52. Duma D, J. C., Cidlowski JA, Multiple glucocorticoid receptor isoforms and mechanisms of post-translational modification. *J Steroid Biochem Mol Biol* **2006,** *102*, 11-21.
53. Kauppi B, J. C., Farnegardh M, Yang J, The three-dimensional structures of antagonistic and agonistic forms of the glucocorticoid receptor ligand-binding domain: RU-486 induces a transconformation that leads to active antagonism. *J Biol Chem* **2003,** *278*, 22748-22754.
54. Nasir, M. S.; Jolley, M. E., Fluorescence polarization: An analytical tool for immunoassay and drug discovery. *Comb Chem High T Scr* **1999,** *2* (4), 177-190.
55. Rossi, A. M.; Taylor, C. W., Analysis of protein-ligand interactions by fluorescence polarization. *Nat Protoc* **2011,** *6* (3), 365-87.
56. Parker, G. J.; Law, T. L.; Lenoch, F. J.; Bolger, R. E., Development of high throughput screening assays using fluorescence polarization: Nuclear receptor-ligand-binding and kinase/phosphatase assays. *J Biomol Screen* **2000,** *5* (2), 77-88.
57. McBee L, C. O., Ion exchange chromatography and electrophoresis of egg yolk. *J Food Sci* **1979,** *44*, 656-660.